SUPPLEMENTAL MATERIAL

Proteasome-Dependent Regulation of Distinct Metabolic States During Long-Term Culture of Human iPSC-Derived Cardiomyocytes

Antje Ebert[1,6,7], Amit U. Joshi[3], Sandra Andorf[4,5], Yuanyuan Dai[1,6,7], Shrivatsan Sampathkumar[1,6,7], Haodong Chen[1,2], Yingxin Li[1,2], Priyanka Garg[1,2], Karl Toischer[6,7], Gerd Hasenfuss[6,7], Daria Mochly-Rosen[3], Joseph C. Wu[1,2]

[1]Stanford Cardiovascular Institute; [2]Department of Medicine, Division of Cardiology; [3]Department of Chemical and Systems Biology; [4]Department of Medicine, Division of Pulmonary and Critical Care Medicine; [5]Sean N. Parker Center for Allergy and Asthma Research, Stanford University School of Medicine, Stanford, CA 94305, USA; [6]Heart Center, University of Göttingen, Department of Cardiology and Pneumology, Robert-Koch-Str. 40, 37075 Göttingen, Germany; [7]DZHK (German Center for Cardiovascular Research), partner site Göttingen, Germany.

SUPPLEMENTAL METHODS

Reprogramming to human iPSCs. The derivation and characterization of the iPSC lines employed in this study are described in previous publications.[1-3] In brief, skin biopsies were obtained from healthy control individuals who consented to donate samples. Dermal fibroblasts were derived from skin biopsies via previously published protocols.[3] Subsequently, cultured fibroblasts were reprogrammed into iPSCs using a lentivirus encoding for the Yamanaka 4 factors (Oct4, Klf4, Sox2, and c-Mcy) as described before.[1-4] These studies and protocols were approved by the Stanford Institutional Review Board. The Stanford Cardiovascular Institute biobank IDs are SCVI20 (C1) and SCVI67 (C2).

Immunofluorescence staining and confocal microscopy. Human iPSC-CMs were passaged 3 days prior to experiment on Matrigel-coated 12-mm glass coverslips. Subsequently, cells were fixed at room temperature for 20 min using 4% PFA in PBS. For subsequent permeabilization, samples were washed with PBS and incubated for 1 hr at room temperature with 0.2 % Triton-X 100 in PBS. Afterward, samples were blocked at room temperature for 2 hr using 5% BSA in PBS, and then stained with mouse anti-human cardiac troponin T (Thermo Scientific and Abcam) and sarcomeric alpha-actinin (Sigma) in 1% BSA-PBS overnight as published previously.[2] Samples were washed with PBS and incubated for 2 hr with a combination of goat anti-mouse Alexa Fluor 594 (Santa Cruz Biotechnology) and DAPI nuclear stain, diluted in 2% BSA-PBS. Coverslips were mounted on glass slides using fluromount G (SouthernBiotech). Pictures were taken with 10x and 40x plan apochromat, and 63x plan apochromat (oil) objectives using a confocal microscope (Carl Zeiss, LSM 510 Meta, Göttingen, Germany) and ZEN software (Carl Zeiss). For immunohistochemistry of established iPSCs, cells were cultured in 6-well plates and processed as

described above. The iPSCs were stained with primary antibodies against OCT3/4, SSEA4, NANOG (all from Santa Cruz Biotechnology, Inc.), and TRA-1-60 (Chemicon).[3] Images of the stained cells were obtained under a brightfield microscope (Leica). Images were analyzed by ImageJ and Adobe Photoshop software.

Microfluidic single-cell quantitative real-time PCR. We previously published a protocol detailing the procedures used here for analysis of single-cell gene expression with microfluidic single-cell quantitative real-time PCR.[5] In brief, cells were dissociated as described above and a single-cell suspension was loaded onto a Fluidigm chip. Following single-cell capture, lysis, and reverse transcription, cDNA samples were loaded onto Biomark 48.48 Dynamic Array chips (Fluidigm). TaqMan Assays (Life Technologies) were utilized for microfluidic quantitative single-cell PCR amplification as listed in Online Tab. I. Duplicate or triplicate PCR reactions was performed for all assay probes. Ct values generated by the BioMark Real-Time PCR software were used for data analysis following normalization to the GAPDH endogenous control gene. Linkage clustering was performed via Euclidian distances.

RNA extraction and quantitative real-time polymerase chain reaction (qRT-PCR). Total RNA was isolated using a miRNeasy mini Kit (Qiagen). Reverse transcription was performed using the iScript cDNA Synthesis Kit (Bio-Rad). For quantitative real-time PCR (qRT-PCR), SYBR™ Green Supermix (Bio-Rad) was utilized based on the manufacturer´s manual. An Applied Biosystems real-time PCR station was used for qRT-PCR detection and recording. Relative mRNA levels were normalized to the 18S mRNA housekeeping control for each reaction. Human and mouse primers utilized in Fig. 1E and Online Fig. ID-G were purchased from IDT, and sequences

are shown in Online Tab. I-II. Human TaqMan probes utilized for single-cell PCR and qRTPCRs shown in Online Fig. VIIA-C were purchased from Thermo Fisher Scientific.

Protein kinase A (PKA) activity assay. Human iPSC-CMs from C1 and C2 cell lines were plated three days prior to the experiment in 6-well plates and treated with PKA inhibitor (H89, 1 uM) or PKA activator (8-CPT, 1 uM) for 24 hr. Cells were lysed at 4 °C and PKA activity was measured using a commercially available kit (Abcam) according to the manufacturer's instructions.

Proteasome activity assay. Human iPSC-CMs from C1 and C2 cell lines were plated three days prior to the experiment in 6-well plates. Cell lysates were prepared as described before[3] and incubated on ice for 60 min with 100 uM DMSO (control vehicle), epoximycin, oleuropein, or PKA inhibitor (H89). The chymotrypsin-like activity of the proteasome was determined using a specific proteasome substrate (N-succinyl-Leu-Leu-Tyr-AMC [LLVY-AMC], Enzo Life Sciences) as described earlier[6] in the presence or absence of ATP (10 uM). Total lysates were incubated with the substrate at room temperature for 60 min. Fluorescence of released LLVY-AMC substrate was measured using a microplate reader system (BioTek).

siRNA knock-down. Human iPSC-CMs from C1 and C2 cell lines were transfected 48 hr before the experiment with siRNAs targeting PKAreg (Thermo Fisher, s286) and Hsp90 (Thermo Fisher, s7000), or non-targeting negative control siRNA (Thermo Fisher, 4390843).

Western blot analysis. Cell lysis and immunoblotting were performed as previously described[3] for analysis of PKA protein levels. Briefly, iPSC-CMs at D30, D90, and D200 were treated as

indicated for 48 hr with chemical modulators (control vehicle/DMSO 100 nM, epoximycin 50 nM, or H89 100 nM) before harvest. Cells were detached using accutase and pelleted at 200 g for 3 min at 4 °C. Cell pellets were resuspended in lysis buffer as described before.[3] Protein concentrations were determined using a BCA kit (Pierce). Antibodies against PKA regulatory subunit (p-PKA IIα reg Antibody (C-5): sc-377575) and PKA catalytic subunit (PKAα cat Antibody (A-2): sc-28315) were purchased from Santa Cruz Biotechnology. Antibodies against phosphorylated PKA (Phospho-PKA C (Thr197) #4781) and Hsp90 (HSP90 (C45G5) Rabbit mAb #4877) was purchased from Cell Signaling Technologies. As a loading control for normalization of detected protein of interest to total protein levels, anti-tubulin (α-Tubulin Antibody #2144) and anti-beta-actin (β-Actin (8H10D10) Mouse mAb #3700) antibodies from Cell Signaling Technology were used. Secondary antibodies were anti-mouse IgG, HRP-linked antibody #7076 and anti-rabbit IgG, HRP-linked antibody #7074 from Cell Signaling Technologies.

Measurement of metabolic viability. Human iPSC-CMs were plated in a 96-well plate format at a cell density of ~80,000 iPSC-CMs per well. Following 48 hr of treatment with chemical modulators as indicated (control vehicle/DMSO 100 nM, epoximycin 50 nM, or H89 100 uM), metabolic viability was measured using an XTT assay (AppliChem) based on the manufacturer´s instructions. The XTT reagent is cleaved to formazan by mitochondrial respiratory chain´s succinate dehydrogenase system (manufacturer´s manual).[7] Because these proteins show activity only in live cells, the XTT assay reflects indirectly both cell viability and mitochondrial succinate dehydrogenase activity.

MitoTracker, MitoSOX, and CellROX assays. Human iPSC-CMs were plated in 96-well plates at a cell density of ~80,000 iPSC-CMs per well. Following 48 hr of treatment with chemical modulators as indicated (control vehicle/DMSO 100 nM, epoximycin 50 nM, or geldanamycin 100 nM), mitochondrial content was quantified via detection of MitoTracker (ThermoFisher) fluorescence at 499 nm based on the vendor´s manual. Mitochondria-specific superoxide was measured using a MitoSOX assay (ThermoFisher) according to the vendor´s protocol. MitoSox detects mitochondrial superoxide via fluorescence of the MitoSox probe at 562 nm. Detection of total cellular reactive oxygen species (ROS) was performed using a CellROX assay (ThermoFisher) based on the manufacturer´s manual. The CellROX probe is a fluorescence-based dye that detects cellular ROS (665 nm).

Measurement of mitochondrial membrane potential. The JC-1 assay (ThermoFisher) was utilized to measure mitochondrial membrane potential (MMP). Human iPSC-CMs were plated either in 96-well plates at a cell density of ~80,000 iPSC-CMs per well for measurement of MMP from live cells, or in 6-well plates for measurement of MMP from isolated mitochondria. Where indicated, cells were treated for 48 hr with chemical modulators (control vehicle/DMSO 100 nM, epoximycin 50 nM, geldanamycin 100 nM or oleuropein 100 nM). Mitochondria were isolated as described earlier.[8] The JC-1 assay was used based on the manufacturer´s instructions. The JC-1 dye displays a potential-dependent localization to mitochondria, which causes a shift in JC-1 fluorescence emission from 525 nm to 590 nm. Data are shown as 590/525 nm fluorescence ratio. A lower 590/525 nm ratio indicates greater mitochondrial membrane depolarization. For cultured cells, signal was normalized using Hoechst staining and fluorescence measurement. For isolated

mitochondrial, equal cell numbers were established prior to cell lysis by counting using a LunaCounter and trypan-blue staining.

Derivation of iPSC-ECs and assessment of LDL uptake. Human iPSC-ECs were differentiated from C1 and C2 lines as described previously.[9] Uptake of low-density lipoprotein (LDL) was detected using 15 μg/ml Dil-acetylated low-density lipoprotein (Life Technologies) for 6 hr as well as a nuclear dye Hoechst. Subsequently, cells were imaged with a brightfield microscope (Leica). Quantification of Dic-LDL uptake was performed using image J software for line C1 (324 cells) and line C2 (227 cells). Normalization of Dic-LDL signal for cell numbers was performed based on nuclear staining (Hoechst).

Contractility analysis. Human iPSC-CMs were plated in 96-well plates at a cell density of ~80,000 iPSC-CMs per well. Following 4 days of culture, drug treatment or siRNA knock-down was performed as indicated. Subsequently, a Sony SI8000 Live Cell Imaging System was utilized to detect and quantify cellular motion via high speed video imaging. Sony SI8000 software was utilized for data analysis.

Microelectrode array recordings. Human iPSC-CMs were plated at 32,000 cells per well on the recording electrode area of the Matrigel-coated 48-well MEA plate and incubated at 37°C in 5% CO_2. The medium was changed two days after plating and MEA recordings were performed 7 days after plating. Electrical activity of iPSC-CMs was recorded via the Maestro recording instrument (Axion BioSystems, USA) at 37 °C using the standard cardiac settings (Axion Biosystems Maestro Axis software). The field potential duration (FPD), defined as the interval between a positive or

negative spike and a subsequent positive deflection, was analyzed with Axion Biosystems software. Fridericia's formula was used to standardize the beat rate-associated dispersed FPD: FPDc = Fridericia's Correction = FPD/(Beat Period)^0.3333.

SUPPLEMENTAL FIGURE LEGENDS

Online Figure I: Characterization of iPSC-CMs at D30, D90 and D200 of culture. (A) Immunohistochemistry analysis of the cardiac markers, sarcomeric alpha actinin (SAA), and cardiac troponin T at D30, D90, and D200. Single cells were imaged with a confocal microscope. Scale bar, 20 μm. **(B)** Quantification of morphological changes during long-term iPSC-CM culture. The number of elongated (e) versus round (r) iPSC-CMs was quantified at D30, D90, and D200 (D30, r=345 and e=134 cells; D90, r=211 and e=319 cells; D200, r=234 and e=605 cells) and is shown as % of total cell number at indicated time points. **(C-H)** Comparison of cardiac developmental markers in iPSC-CMs at D30, D90, and D200, as well as in mouse heart tissue at postnatal days P1-2, P30, and P180. Indicated mRNA expression was analyzed via qRT-PCR for human and mouse qRT-PCR primers. mRNA expression data for human iPSC-CMs are shown as fold-change of D30. mRNA expression data from murine heart tissue are shown as fold-change of P1-2. Human iPSC-CMs, n=2 independent cell lines per group and murine heart tissue, n=3 animals per group. Data are expressed as mean ± s.e.m. $*P < 0.05$, $**P < 0.01$, $***P < 0.001$, as calculated by Student's t-test.

Online Figure II: Characterization of iPSCs and iPSC-CMs. (A) Immunohistochemistry for expression of the pluripotency markers Oct4, SOX2, TRA-8-81, Nanog, SSEA4, and TRA-1-60 in iPSCs. Scale bar, 20 μm. **(B-C)** Expression of cardiac-specific markers is shown in D30 iPSC-CMs as fold-change of iPSCs via single-cell RT-PCR for n=2 cell lines **(B)** and by immunohistochemistry for sarcomeric alpha-actinin, cardiac troponin T, and myosin light chain 2a **(C)**. Scale bar, 20 μm.

Online Figure III: Baseline electrophysiological properties of iPSC-CMs. Electrophysiological parameters of interest were analyzed by multielectrode arrays (MEAs) in iPSC-CMs at D30. **(A)** Field potentials recorded via MEAs (D30 iPSC-CMs). A representative raw trace denotes field potential duration (FDP), T-wave, and beat period over time. **(B)** Averages of iPSC-CM field potential parameters obtained via MEAs (D30). Data are expressed as mean ± s.e.m., n=2 independent cell lines per group.

Online Figure IV: Microfluidic single-cell PCR profiling of distinct metabolic and structural changes during long-term culture of iPSC-CMs. Dot-plot diagrams show expression profiles for 47 genes assessed by quantitative single-cell PCR after 30, 90, and 200 days of prolonged culture. Expression levels are shown as Ct values and compared to iPSCs. Expression analysis normalized per cell for iPSCs and day 30, day 90, and day 200 iPSC-CMs. Data are shown for n=2 independent cell lines per group.

Online Figure V: Intra-group comparisons following transcriptomic profiling. (A) PCA for transcriptomic expression detected in D30, D90, and D200 iPSC-CMs. **(B)** Heatmap showing a pairwise comparison with unsupervised clustering of significantly differentially expressed (SDE) transcripts at D90 versus all others at D30 and D200. **(C)** Intra-group comparisons showing upregulation and downregulation of significantly changed genes between D90 versus D200 and D30 versus D200. Directional changes are marked in blue (decrease of expression) and red (increase of expression). **(D)** Decrease of fetal-like gene expression from D30 to D90 and D200 **(E)** Increase of expression for genes relating to oxidative phosphorylation and beta-oxidation from D30 to D90 and D200. Data shown for n=2 independent cell lines per group.

Online Figure VI: Functional interaction network analysis predicts PKA-mediated regulation of TNNI3 as a critical component in the intra-group comparisons of D200 vs D30 and D200 vs D90. (A) IPA of AmpliSeq transcriptomic data generated the functional interaction network for the intra-group comparison of early versus very late time points. The shown IPA network displays regulatory connections for the comparison of D200 vs D30 and D200 vs D90. **(B)** Significantly changed genes overlapping among D30, D90, and D200 as identified via transcriptomic profiling (top row) and single-cell PCR (bottom row). **(C-D)** Upregulation of PKA- and cAMP-mediated signaling. Significant changes in **(C)** cAMP-mediated signaling and **(D)** PKA-mediated signaling are shown as –log(p-value), as analyzed by IPA. *NS*, not significant. Data shown for n=2 independent cell lines per group.

Online Figure VII: Validation of pathway components related to distinct regulation of metabolic turnover during long-term culture of iPSC-CMs. Quantification of differentially expressed genes (DEGs) in mitochondrial metabolism previously identified by genomic sequencing and IPA. Shown is the [log] mRNA expression as fold-change for indicated genes in D30, D90, and D200 iPSC-CMs as analyzed by qRT-PCR for **(A)** oxidative stress as well as redox scavenging and **(B)** mitochondrial metabolism. (**C**) Numerical values for data shown in **(A)** and **(B)**. Data are expressed as mean ± s.e.m., n=2 independent cell lines per group.

Online Figure VIII: Upregulation of metabolic function in long-term cultured iPSC-CMs is not dependent on cellular redox stress. (A) Mitochondrial content is quantified via detection of MitoTracker (Life Technologies) fluorescence at 499 nm for iPSC-CMs at the indicated time points. **(B)** Following long-term culture, reduced mitochondrial levels of reactive oxygen species

(ROS) are observed. Mitochondrial superoxide is measured via fluorescence of the Mitosox probe (Life Technologies) at 562 nm. Data are expressed as mean ± s.e.m., n=2 independent cell lines as well as 2 independent experiments per group, *P <0.05, **P <0.01, ns = not significant, as calculated by Student's t-test.

Online Figure IX: Motion imaging analysis of iPSC-CMs shows increasing velocity and duration of contraction at the late time point. Using a Sony motion imaging analysis station (SI8000), contraction in beating iPSC-CMs was analyzed at D30, D90, and D200. Increased contraction velocity and duration at the late time point were detected. **(A)** Motion-traction graph generated by the SI8000 software showing start of contraction, contraction peak and end, as well as relaxation peak and end. **(B)** Contraction velocity and **(C)** contraction duration as analyzed using SI8000 motion analysis software. Data are expressed as mean ± s.e.m., n=2 independent cell lines per group, *P <0.05, **P <0.01, as calculated by Student's t-test.

Online Figure X: Concomitantly differential HSP- and ubiquitin-related, but not proteasome-related transcript levels, in distinct metabolic stages during long-term cultured iPSC-CMs. (A) Transcriptomic sequencing revealed no significant changes in expression of proteasome-encoding genes. Data are shown for n=2 independent cell lines per group. **(B-C)** Epoximycin treatment does not affect mitochondrial content or mitochondrial ROS production at any of the indicated time points. **(B)** Shown is mitochondrial content measured via MitoTracker in live iPSC-CMs at indicated time points and **(C)** mitochondrial ROS measured via MitoSOX in iPSC-CMs at indicated time points. Data are expressed as a ratio of epoximycin treatment divided by control vehicle. Data are displayed as mean ± s.e.m., n=2 independent cell lines as well as 2

independent experiments per group. **(D)** Relative mRNA expression as detected by transcriptomic sequencing for heat shock protein (HSP) chaperones. **(E)** Heatmaps showing the expression changes for ubiquitin-related genes detected in transcriptomic sequencing at indicated time points. Left panel, differentially expressed genes during long-term culture. Right panel, no significant change. Data are shown for n=2 independent cell lines per group.

Online Figure XI: Distinct metabolic stages during long-term culture of iPSC-CMs depend on cAMP-PKA regulation at D30 and D200, but not at D90. (A) Relative mRNA expression detected in genomic sequencing for PKA-related transcripts PRKACA and PRKAR1A. Data are shown for n=2 independent cell lines per group. **(B)** Epoximycin-based proteasomal inhibition does not alter PKA activity. **(C)** Effect of oleuropein (Ole) on proteasome activity. Measurement of fluorescence activity of the proteasome-specific molecule Suc-LLVY-AMC is detected following hydrolysis at 354 nm. Data are expressed as mean ± s.e.m., n=2 independent cell lines as well as 2 independent experiments per group. $*P < 0.05$, $**P < 0.01$, as calculated by Student's t-test. **(D)** Cellular cAMP levels are detected in iPSC-CMs at indicated time points via the cAMP-Glo assay kit (Promega). **(E)** Changes in proteasome activity at different time points following of addition of cAMP (10 nM), compared to control vehicle (DMSO 10 nM) at each time point. Shown are averages of n=2 cell lines for 20S and 26S proteasome, Mann-Whitney testing and Dunn´s post-hoc test were performed. For both 20S and 26S, ns = not significant for D30 vs D90 baseline (control vehicle) and $***P < 0.001$ for D30 vs D200 and D90 vs D200 baseline (control vehicle). **(F-G)** Human iPSC-CMs at indicated time points were cultured for 24 hr in presence of DMSO (control vehicle) or indicated chemical modulators. Metabolic viability was measured using the XTT reagent in iPSC-CMs in presence or absence of FCCP, a respiratory chain uncoupler. XTT

cleavage by mitochondrial respiratory chain´s succinate dehydrogenase system results in absorbance detected at 450 nm (relative units). **(F)** Changes in cellular metabolic viability, reflected in XTT cleavage by mitochondrial respiratory chain´s succinate dehydrogenase system in presence or absence of PKA activation (8-CPT), were determined at D30, D90, or D200 (absorbance detected at 450 nm, relative units). **(G)** Changes in cellular metabolic viability, reflected in XTT cleavage by mitochondrial respiratory chain´s succinate dehydrogenase system, were measured in presence or absence of 10 nM cAMP at D30, D90, or D200 (absorbance detected at 450 nm, relative units). **(H)** Assessment of mitochondrial membrane potential (MMP) via a potential sensor dye, JC-1; shown are 590/525 nm fluorescence ratios. Mitochondria were isolated from D30 iPSC-CMs, and 590/525 nm fluorescence ratios are shown. Potential-dependent localization of JC-1 to mitochondria causes a shift in JC-1 fluorescence emission from 525 nm to 590 nm. Data are expressed as mean ± s.e.m., n=2 independent cell lines as well as 2 independent experiments per group. **P* <0.05, ***P* <0.01, as calculated by Student's t-test. For **(D-G)**, Mann-Whitney testing and Dunn´s post-hoc test or Student´s t-test and Sidak´s post-hoc test were performed. **P* <0.05, ***P* <0.01, ****P* <0.001. Data are expressed as mean ± s.e.m., n=2 independent cell lines per group.

Online Figure XII: Hsp90 is downregulated following long-term culture. (A) Immunoblot-based analysis of Hsp90 expression in iPSC-CMs at indicated time points and in lysates from human heart tissue. Tubulin and β-actin were used as loading controls where indicated. **(B)** Quantification of **(A)**. Data are expressed as mean ± s.e.m. and shown for n=2 independent cell lines as well as n=4 human hearts. **(C)** Immunoblot analysis of mouse heart tissue at postnatal days P1-2, P30, and P180 showing the protein expression levels at indicated time points for Hsp90 as

well as phospho-PKA, PKAcat, and PKAreg. Tubulin was used as a loading control. **(D-G)** Quantification of **(C)**. Data are expressed as mean ± s.e.m. and shown for n=3 animals per group.

Online Figure XIII: Validation of siRNA-mediated knock-down of PKAreg and Hsp90. Cell lysates were analyzed following 48 hr of siRNA knock-down via immunoblot for silencer control siRNA (siRNA control) and two different siRNAs targeting **(A)** PKAreg and **(B)** Hsp90. Data are normalized for loading control (β-actin) and shown for n=2 independent cell lines.

Online Figure XV: Motion imaging analysis of iPSC-CMs shows increasing velocity and duration of contraction following activation of PKA or inhibition of Hsp90. Contraction in beating iPSC-CMs was analyzed at D30 using a Sony motion imaging analysis station (SI8000). **(A-B)** Human iPSC-CMs were subjected to 48 hr of siRNA knock-down using silencer control siRNA (siRNA control) or siRNA targeting either PKA regulatory subunit (siRNA PKAreg) or Hsp 90 (siRNA Hsp90). Shown are **(A)** contraction velocity and **(B)** contraction duration as analyzed by SI8000 motion analysis software. **(C-D)** Human iPSC-CMs were treated for 96 hr with 50 nM DMSO (control vehicle), geldanamycin (gelda), or 8-CPT as indicated. Shown are **(C)** contraction velocity and **(D)** contraction duration analyzed using SI8000 motion analysis software. Data are expressed as mean ± s.e.m., n=2 independent cell lines per group.

Online Figure XVI: Hsp90 inhibition does not alter mitochondrial content or ROS production in human iPSC-ECs. Human iPSC-ECs were cultured for 48 hr in presence of 50 nM DMSO (control vehicle), geldanamycin (gelda) or epoximycin (epoxi) as indicated. **(A)** Detection of total mitochondrial content based on fluorescence (580 nm) of MitoTracker (Life

Technologies), a mitochondria-specific fluorescent dye. **(B)** Detection of mitochondrial reactive oxygen species (ROS) via MitoSOX (Life Technologies), a fluorescence-based dye that detects mitochondrial superoxide (516 nm). **(C)** Detection of total cellular reactive oxygen species (ROS) using CellROX deep red (Life Technologies). Data are expressed as mean ± s.e.m., n=2 independent cell lines as well as 2 independent experiments per group are shown.

SUPPLEMENTAL TABLES

Online Table I: Human qRTPCR primers (relating to Fig. 1 and Online Fig. I)

Human primers as utilized in Fig. 1E and Online Fig. ID-G are shown and were purchased from IDT.

Online Table II: Mouse qRTPCR primers (relating to Online Fig. I)

Mouse primers as utilized in Online Fig. IID-G are shown and were purchased from IDT.

Online Table III: Human TaqMan probes utilized for singe-cell PCR (ThermoFisher)

Relating to Fig. 2, Online Fig IV, and Online Fig. VIIA

Human TaqMan probes utilized for single-cell PCR and qRTPCRs as shown in Fig. 2, Online Fig. IV and Online Fig. VIIA-C were purchased from ThermoFisher.

Online Table IV: Pathway analysis via STRING database (Relating to Fig. 5A)

Functional interaction network analysis predicts PKA-mediated regulation as a critical component in the intra-group comparisons for D200 vs D30 and D200 vs D90. Interactome mapping for PKA using the STRING database. Relevant interaction partners previously identified via transcriptomic sequencing and IPA pathway mapping to be significantly changed at D90 and D200 (D90 vs D200) are highlighted in orange in Fig. 5A. Shown is the STRING database assignment of these interactors to the first shell and second shell or interaction partners (interactors). Data shown for n=2 independent cell lines per group.

SUPPLEMENTAL MOVIES

Beating monolayer of D30, D90, and D200 iPSC-CMs. Beating monolayers of iPSC-CMs were recorded at indicated time points at 20x magnification using a Leica camera and brightfield microscope.

Online Movie I: D30

Online Movie II: D90

Online Movie III: D200

SUPPLEMENTAL REFERENCES

1. Sun N, Yazawa M, Liu J, Han L, Sanchez-Freire V, Abilez OJ, Navarrete EG, Hu S, Wang L, Lee A, Pavlovic A, Lin S, Chen R, Hajjar RJ, Snyder MP, Dolmetsch RE, Butte MJ, Ashley EA, Longaker MT, Robbins RC and Wu JC. Patient-specific induced pluripotent stem cells as a model for familial dilated cardiomyopathy. *Sci Transl Med*. 2012;4:130ra47.

2. Lan F, Lee AS, Liang P, Sanchez-Freire V, Nguyen PK, Wang L, Han L, Yen M, Wang Y, Sun N, Abilez OJ, Hu S, Ebert AD, Navarrete EG, Simmons CS, Wheeler M, Pruitt B, Lewis R, Yamaguchi Y, Ashley EA, Bers DM, Robbins RC, Longaker MT and Wu JC. Abnormal calcium handling properties underlie familial hypertrophic cardiomyopathy pathology in patient-specific induced pluripotent stem cells. *Cell Stem Cell*. 2013;12:101-13.

3. Ebert AD, Kodo K, Liang P, Wu H, Huber BC, Riegler J, Churko J, Lee J, de Almeida P, Lan F, Diecke S, Burridge PW, Gold JD, Mochly-Rosen D and Wu JC. Characterization of the molecular mechanisms underlying increased ischemic damage in the aldehyde dehydrogenase 2 genetic polymorphism using a human induced pluripotent stem cell model system. *Sci Transl Med*. 2014;6:255ra130.

4. Chen G, Gulbranson DR, Hou Z, Bolin JM, Ruotti V, Probasco MD, Smuga-Otto K, Howden SE, Diol NR, Propson NE, Wagner R, Lee GO, Antosiewicz-Bourget J, Teng JM and Thomson JA. Chemically defined conditions for human iPSC derivation and culture. *Nat Methods*. 2011;8:424-9.

5. Sanchez-Freire V, Ebert AD, Kalisky T, Quake SR and Wu JC. Microfluidic single-cell real-time PCR for comparative analysis of gene expression patterns. *Nat Protoc*. 2012;7:829-38.

6. Hamouda MA, Belhacene N, Puissant A, Colosetti P, Robert G, Jacquel A, Mari B, Auberger P and Luciano F. The small heat shock protein B8 (HSPB8) confers resistance to

bortezomib by promoting autophagic removal of misfolded proteins in multiple myeloma cells. *Oncotarget*. 2014;5:6252-66.

7. Roehm NW, Rodgers GH, Hatfield SM and Glasebrook AL. An improved colorimetric assay for cell proliferation and viability utilizing the tetrazolium salt XTT. *J Immunol Methods*. 1991;142:257-65.

8. Budas GR, Churchill EN, Disatnik MH, Sun L and Mochly-Rosen D. Mitochondrial import of PKCepsilon is mediated by HSP90: a role in cardioprotection from ischaemia and reperfusion injury. *Cardiovasc Res*. 2010;88:83-92.

9. Gu M, Shao NY, Sa S, Li D, Termglinchan V, Ameen M, Karakikes I, Sosa G, Grubert F, Lee J, Cao A, Taylor S, Ma Y, Zhao Z, Chappell J, Hamid R, Austin ED, Gold JD, Wu JC, Snyder MP and Rabinovitch M. Patient-specific iPSC-derived endothelial cells uncover pathways that protect against pulmonary hypertension in BMPR2 mutation carriers. *Cell Stem Cell*. 2017;20:490-504 e5.

Online Figure I

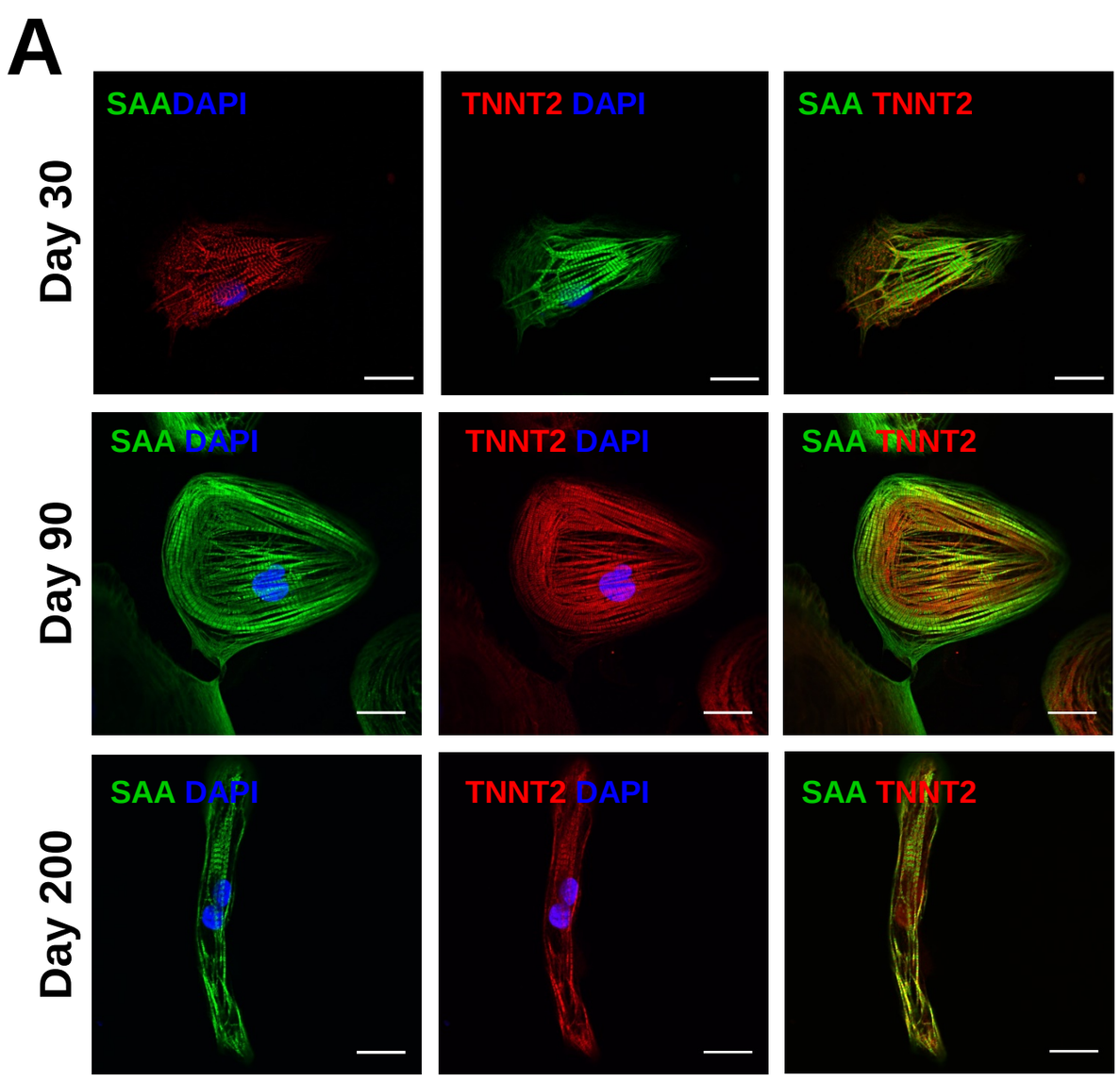

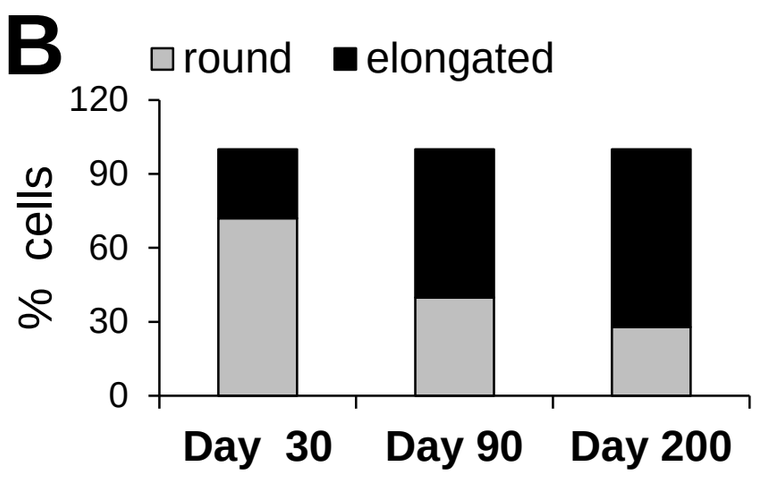

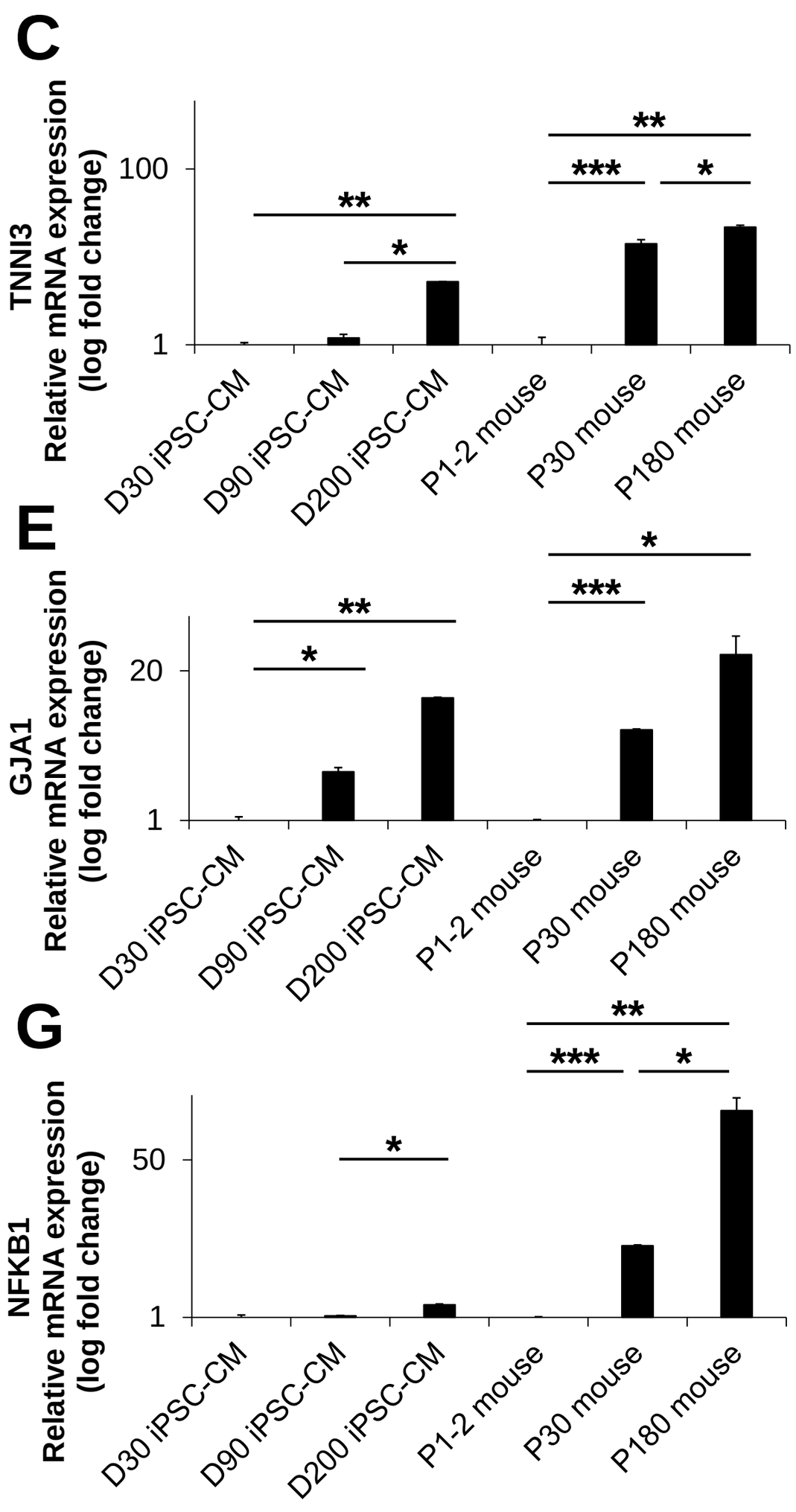

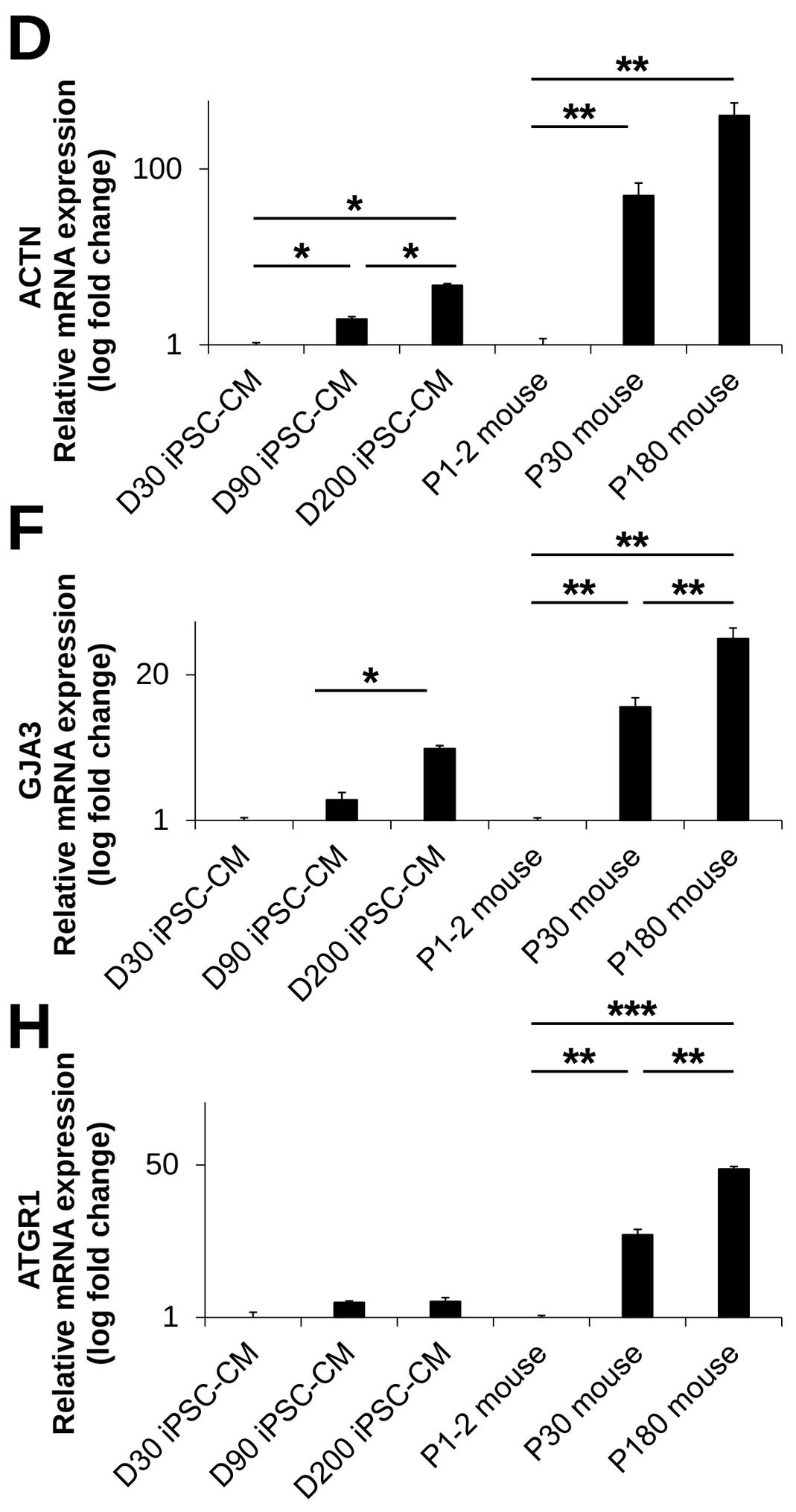

Online Figure II

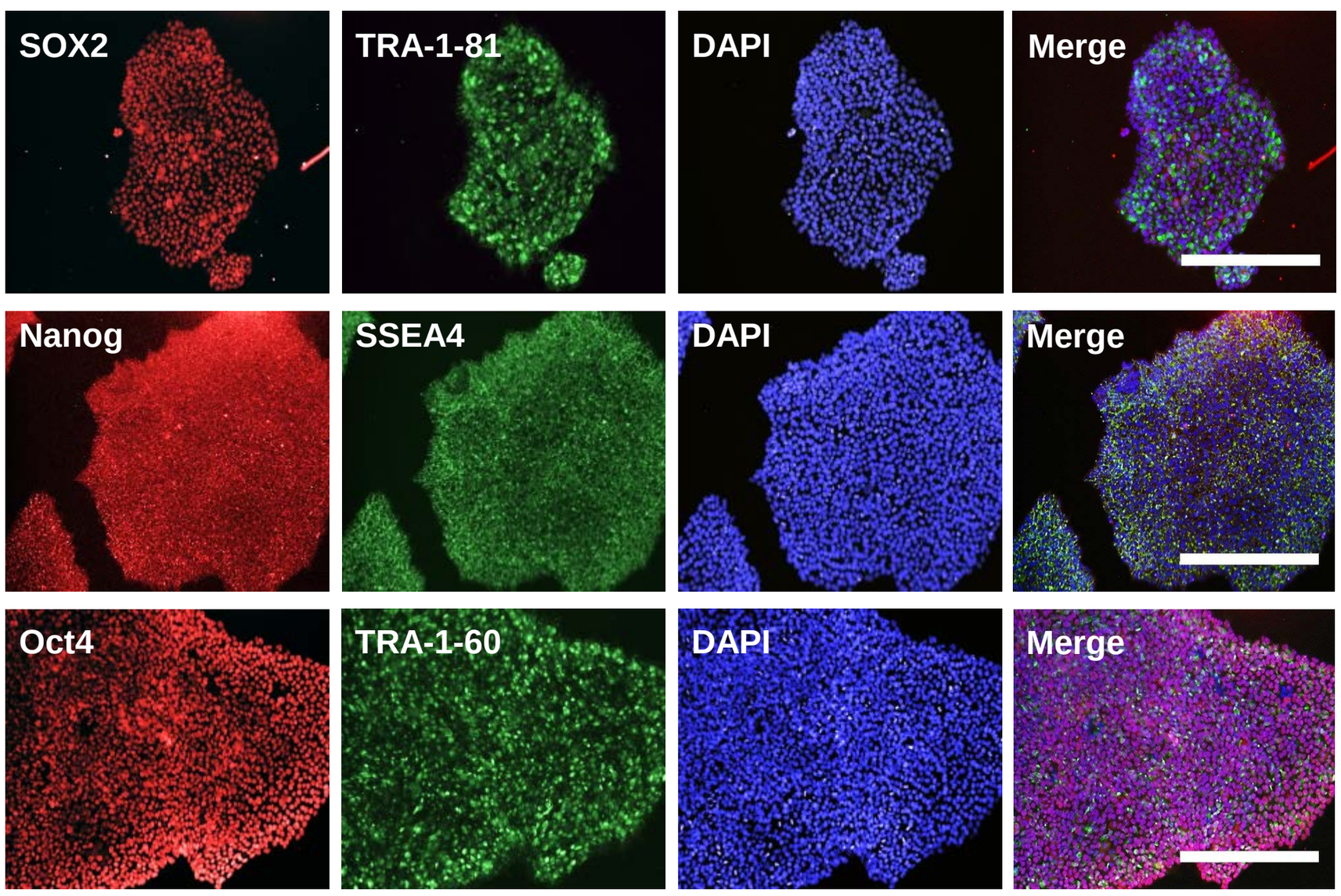

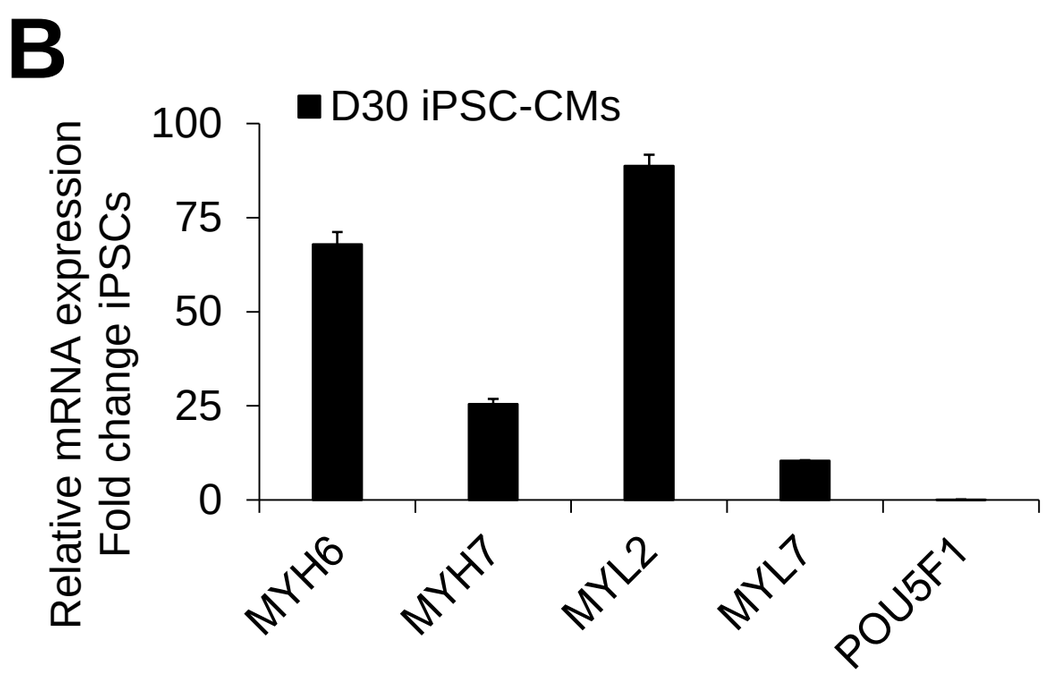

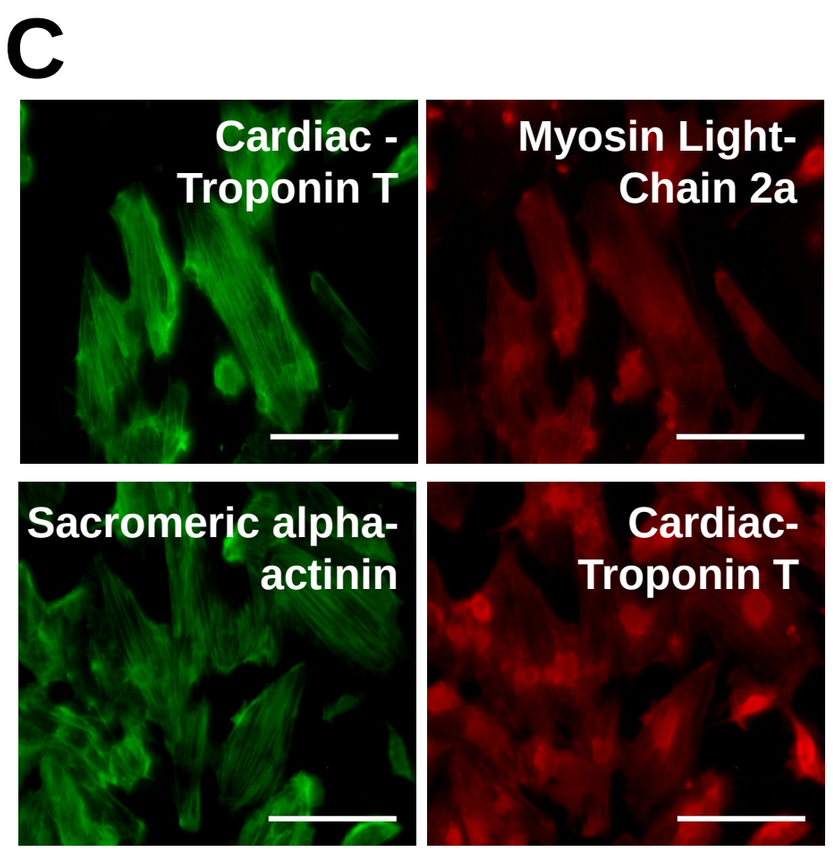

Online Figure III

A

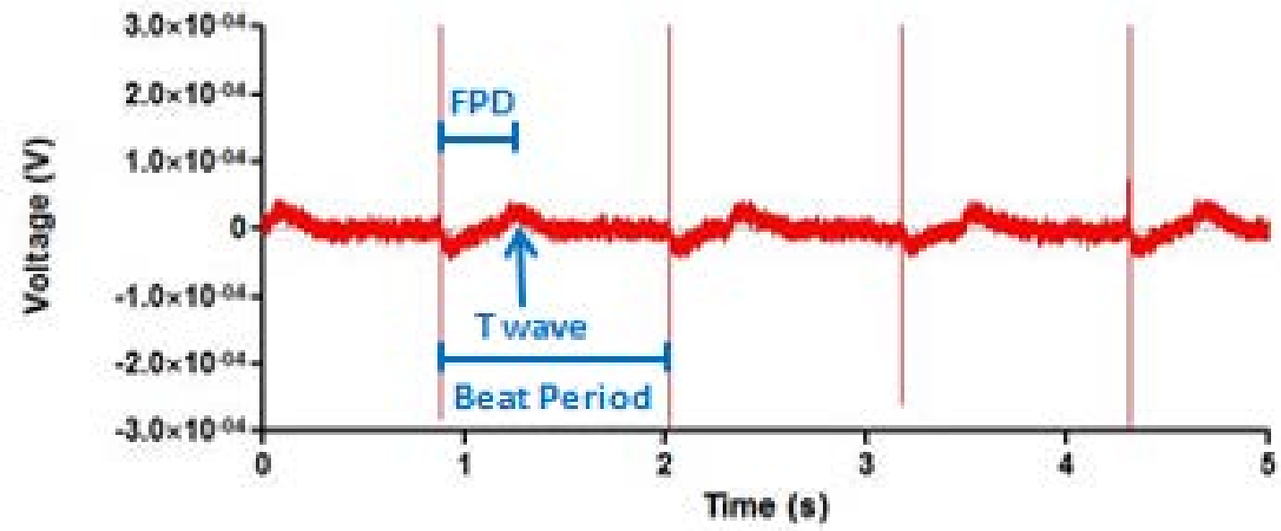

B

iPSC-CM monolayer	Beat Rate (bpm)	FPD (ms)	FPDc (ms)	Beat period (s)
n=7	51.5 ± 1.95	361.3 ± 42.3	342.4 ± 38.9	1.18 ± 0.1

Online Figure IV

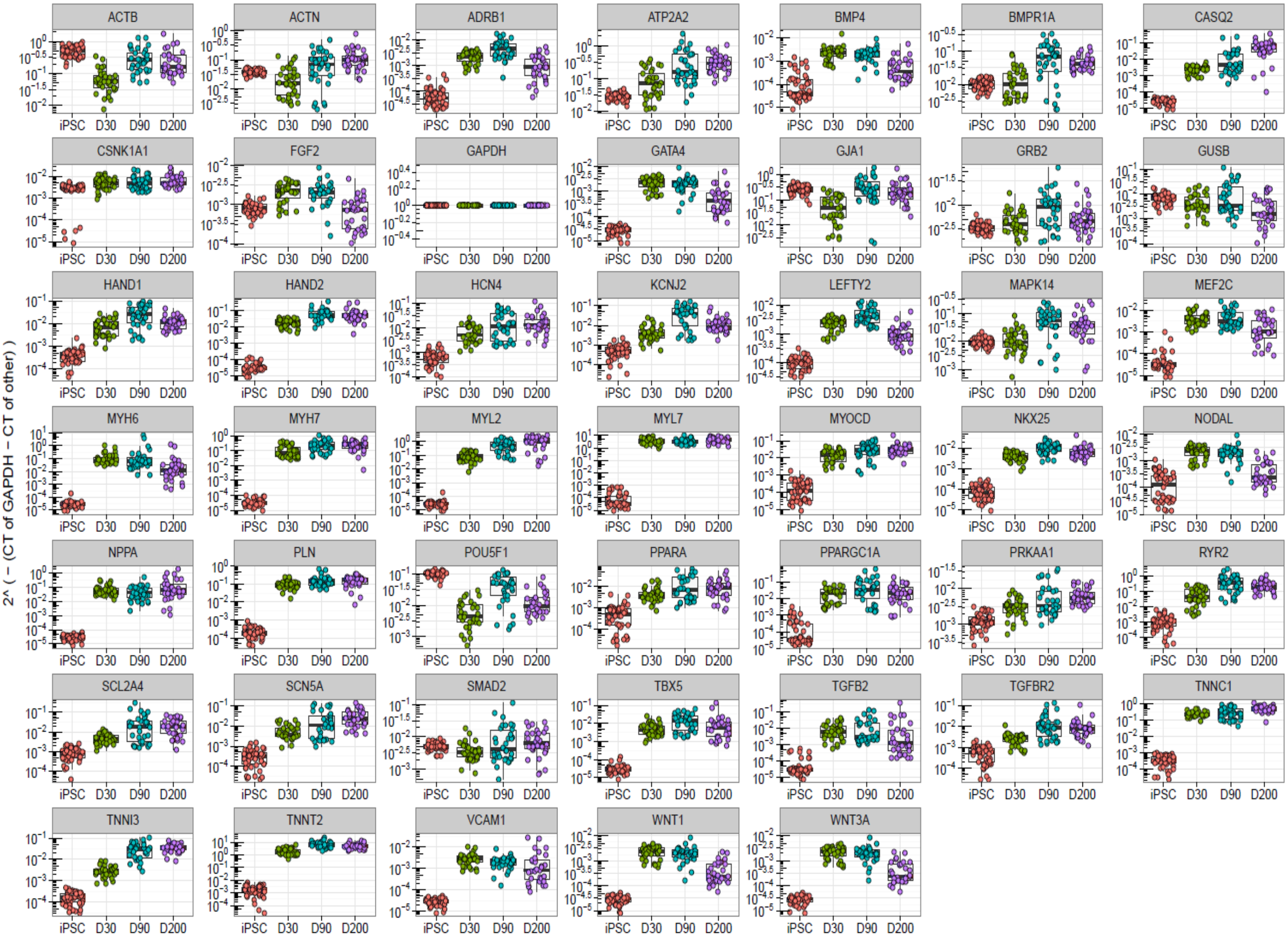

Online Figure V

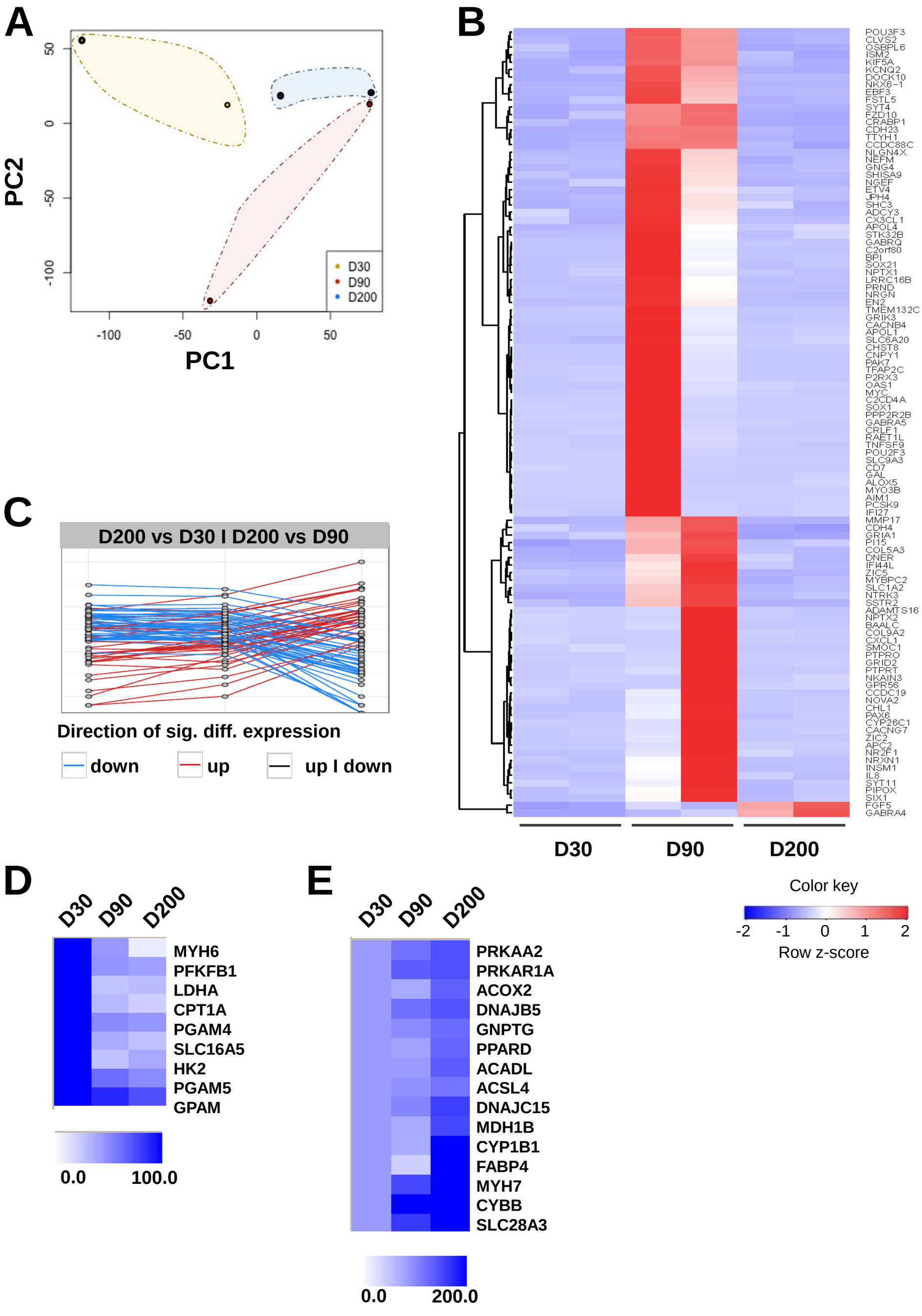

Online Figure VI

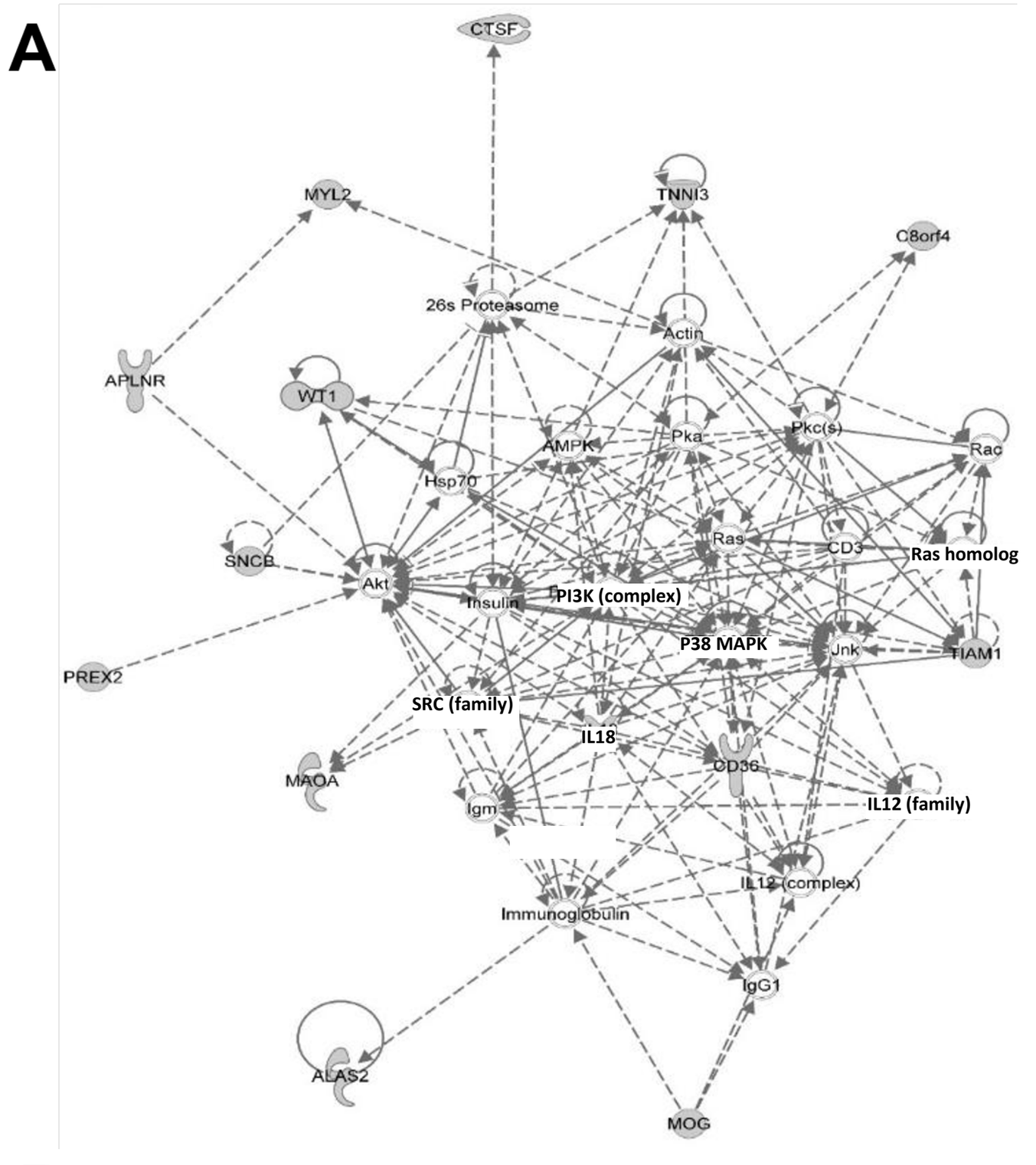

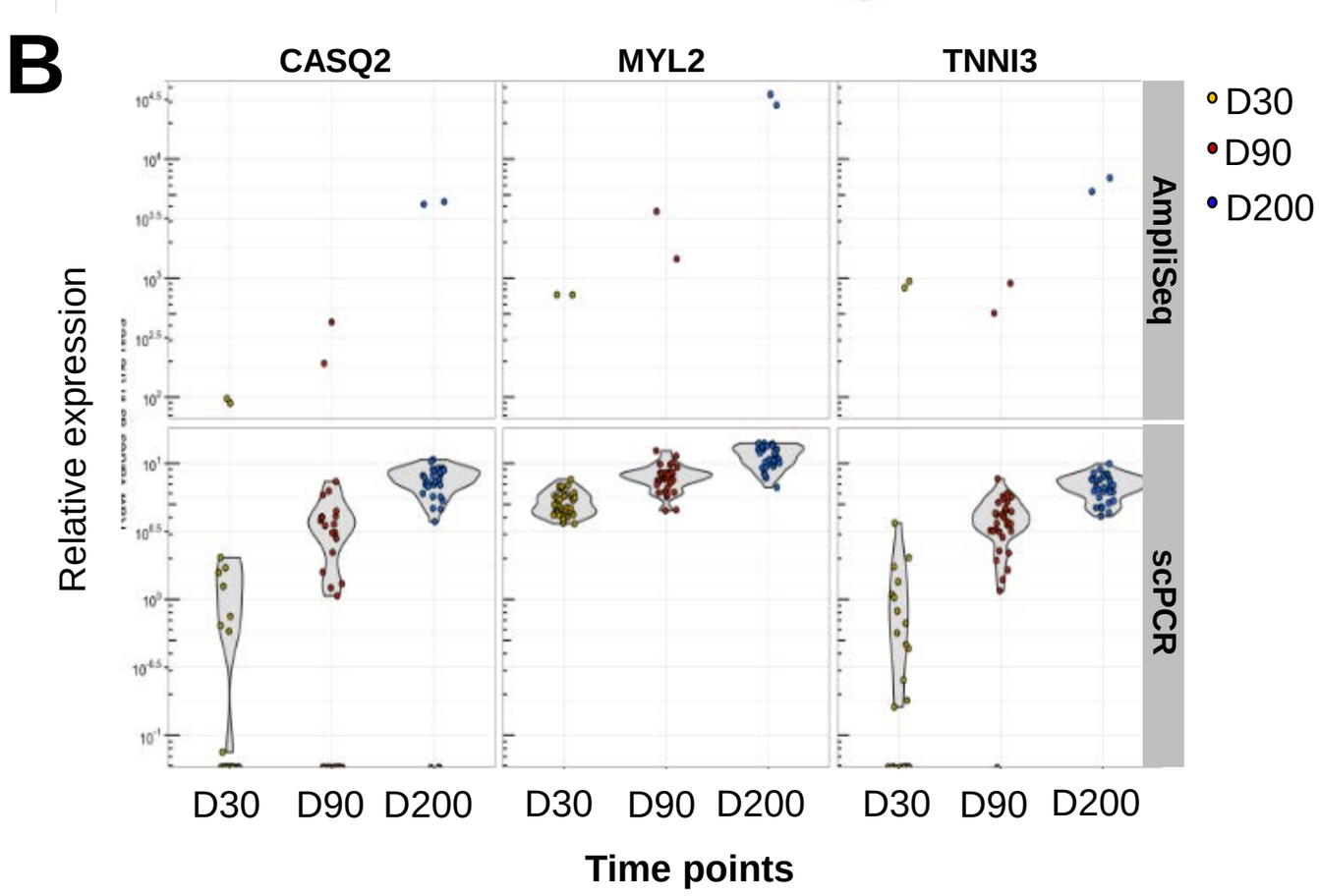

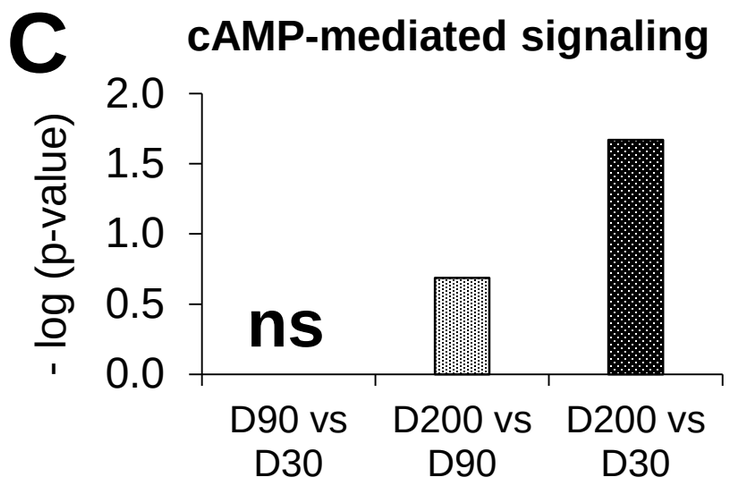

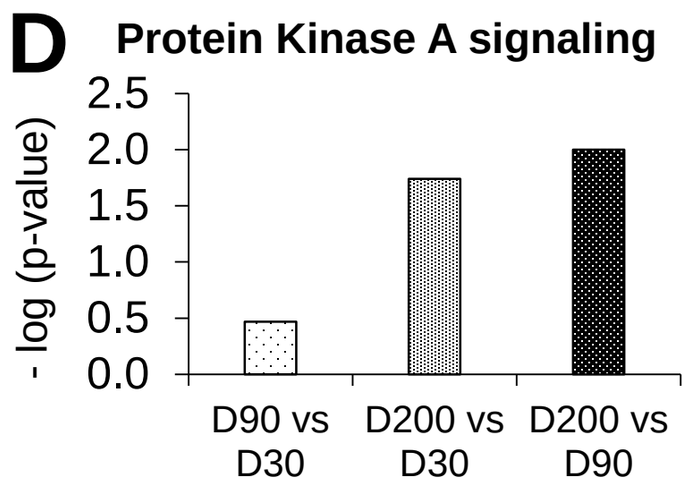

Online Figure VII

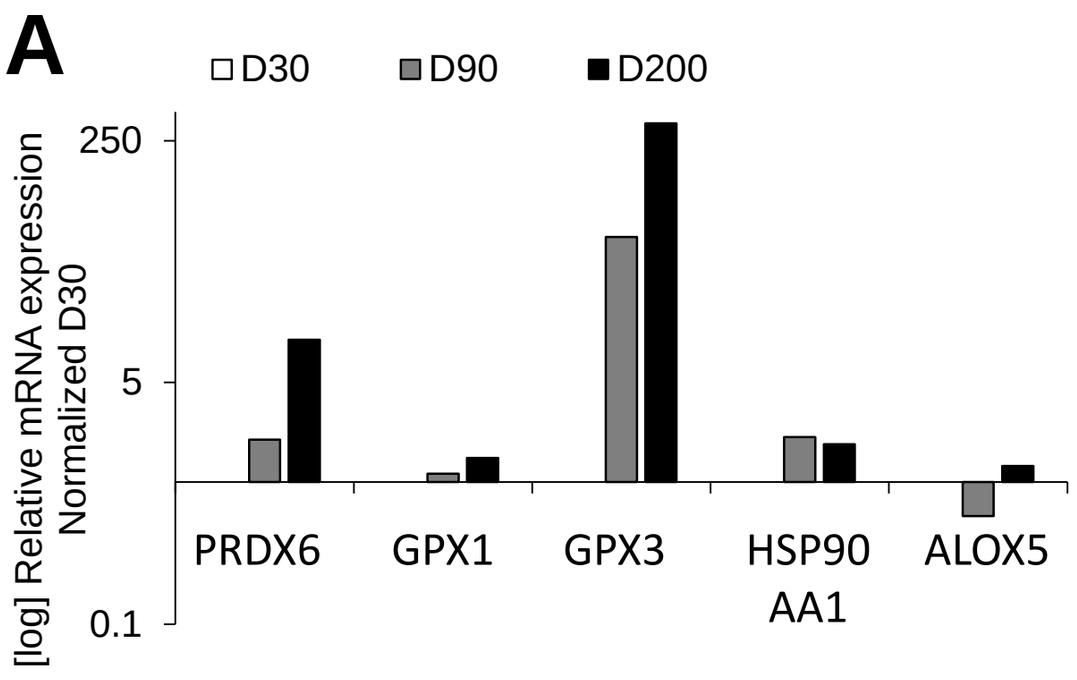

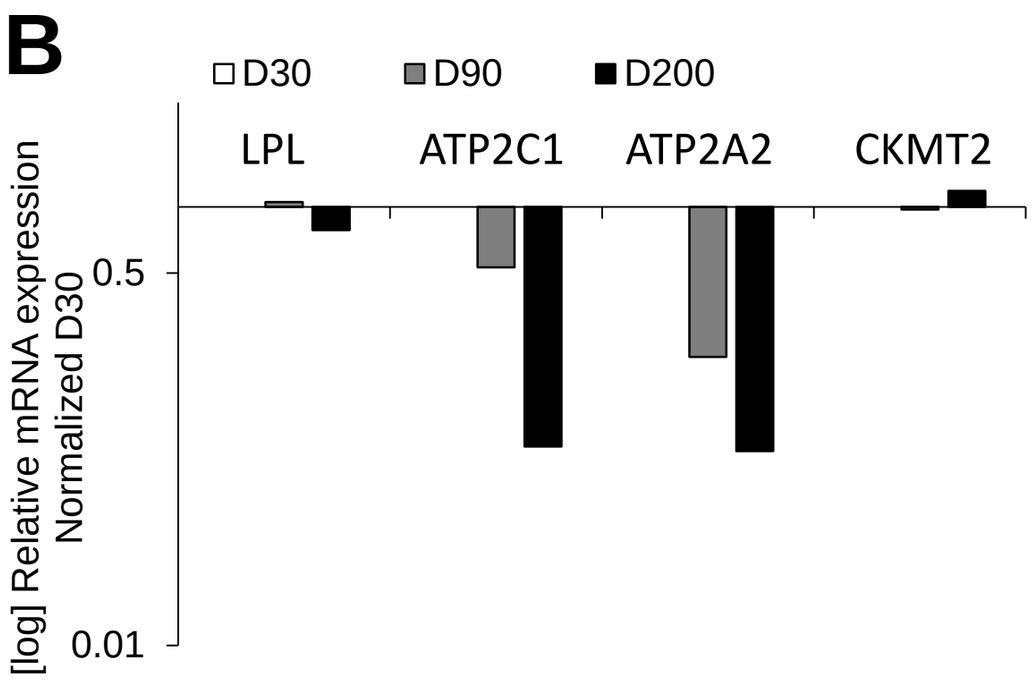

C

[log] Relative mRNA expression, normalized to D30						
Gene ID	**D30**	**SEM**	**D90**	**SEM**	**D200**	**SEM**
PRDX6	1	2E-06	1.9838	0.008	9.979	0.0237
GPX1	1	0.012	1.1404	0.017	1.473	0.0146
GPX3	1	3E-05	52.707	0.681	331.8	0.0114
HSP90AA1	1	8E-07	2.0643	0.004	1.838	0.0389
ALOX5	1	0.002	0.5765	0.001	1.297	0.0021
LPL	1	0.011	1.0538	0.012	0.784	0.0012
ATP2C1	1	0.029	0.5308	0.007	0.081	0.0152
ATP2A2	1	0.048	0.2073	0.004	0.077	0.0144
CKMT2	1	0.038	0.9745	2E-06	1.186	2E-05

Online Figure VIII

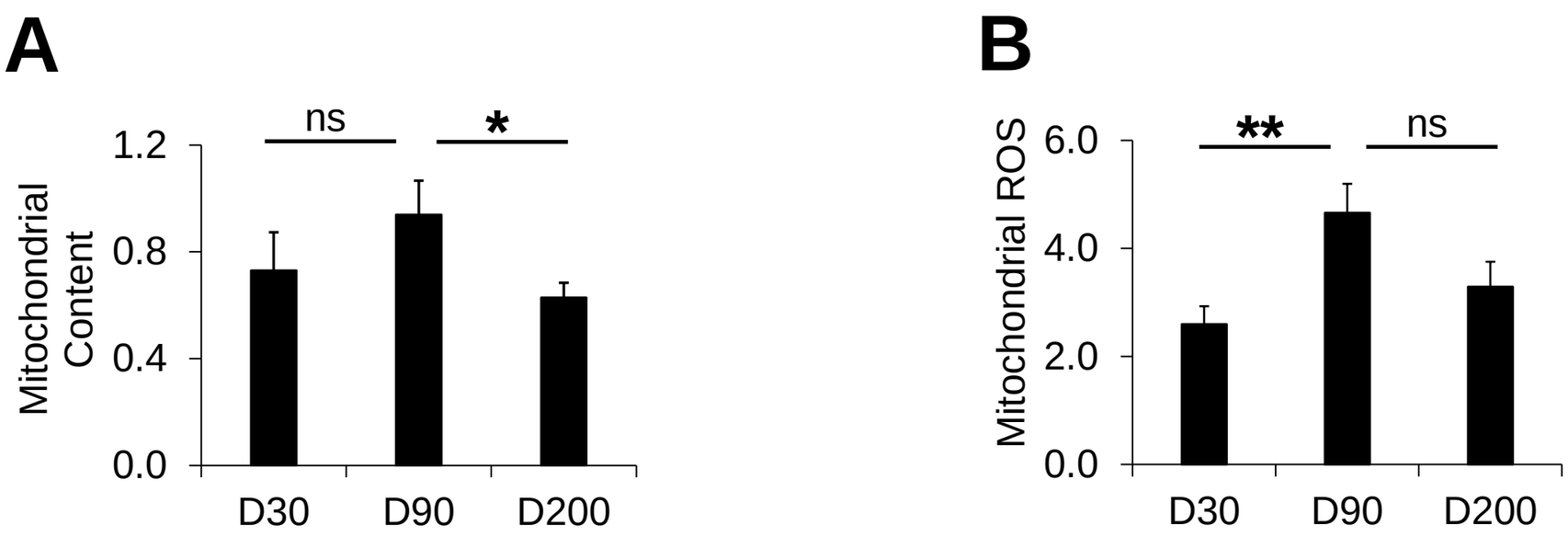

Online Figure IX

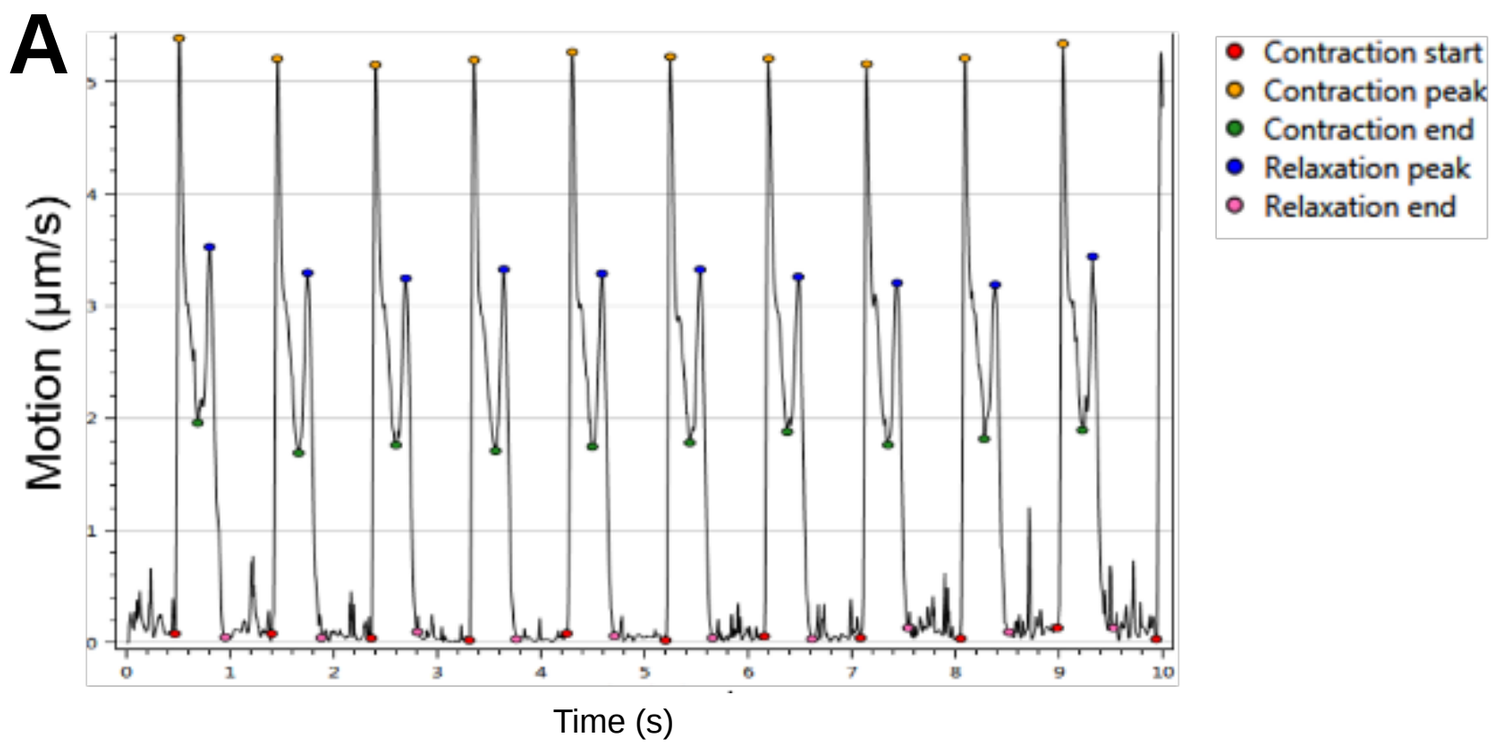

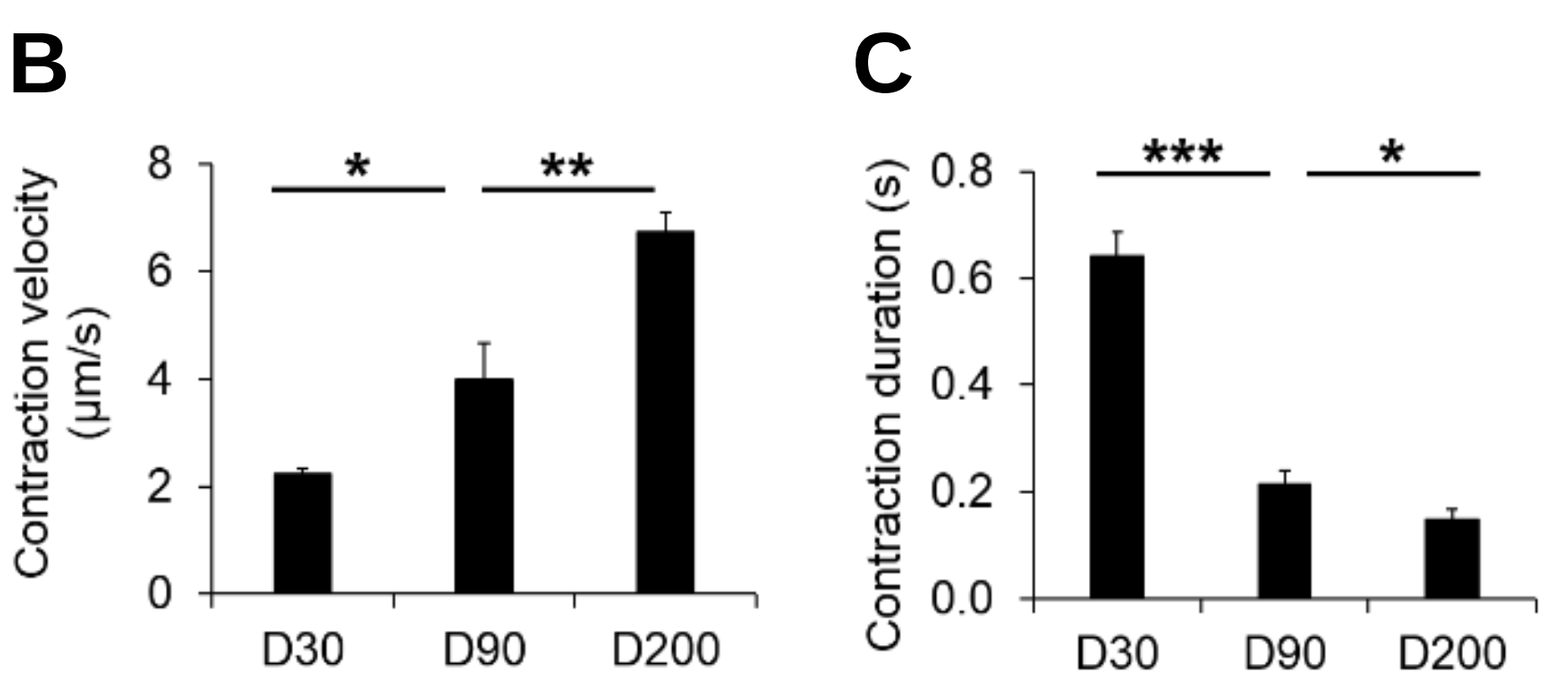

Online Figure X

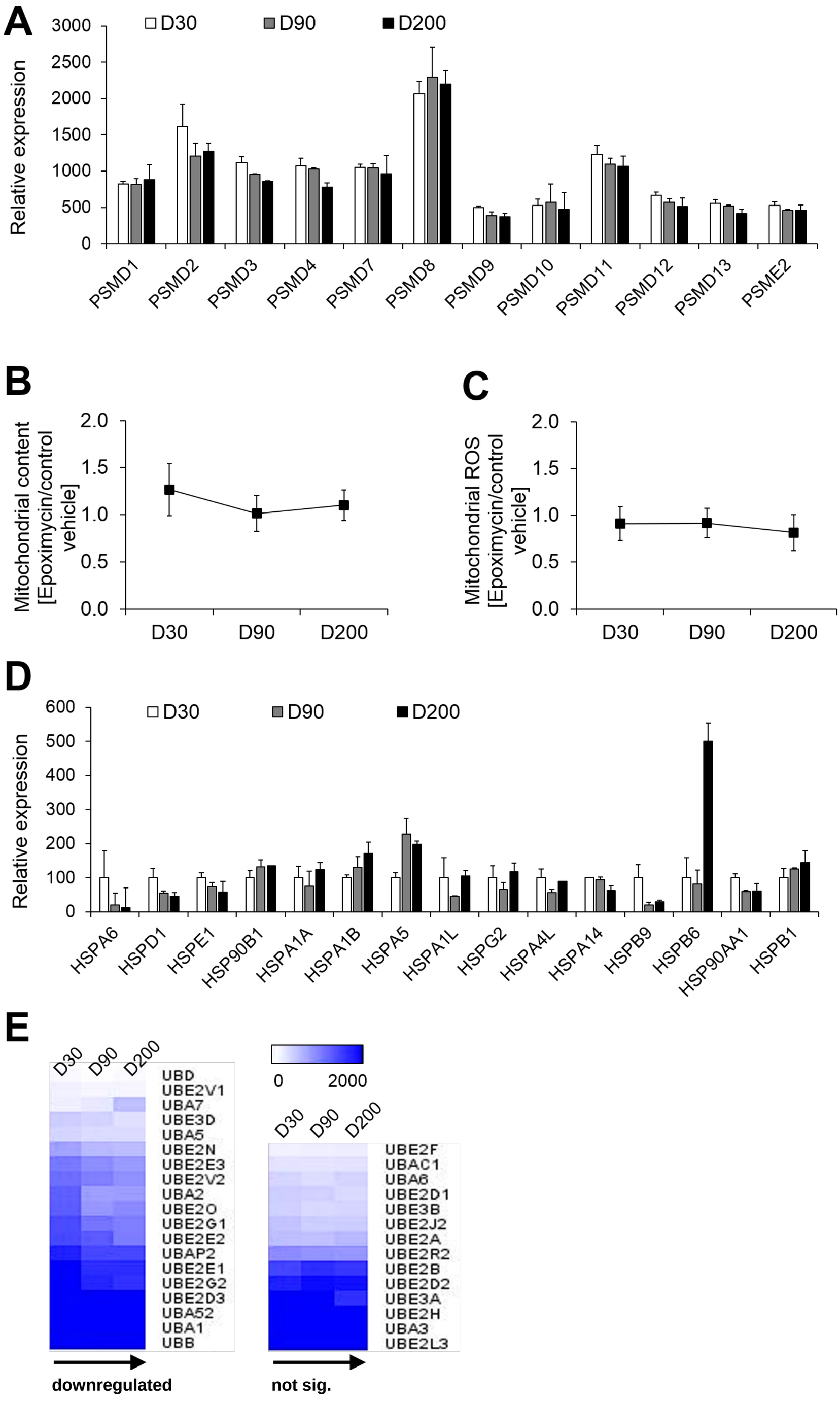

Online Figure XI

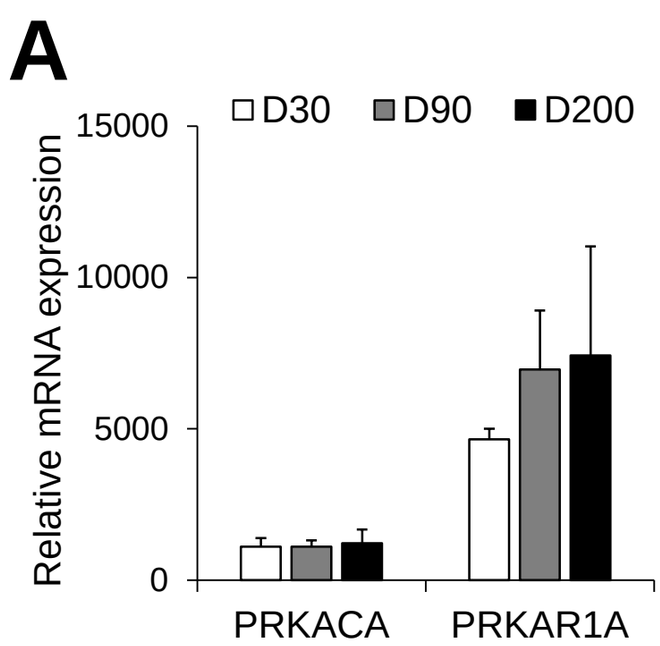

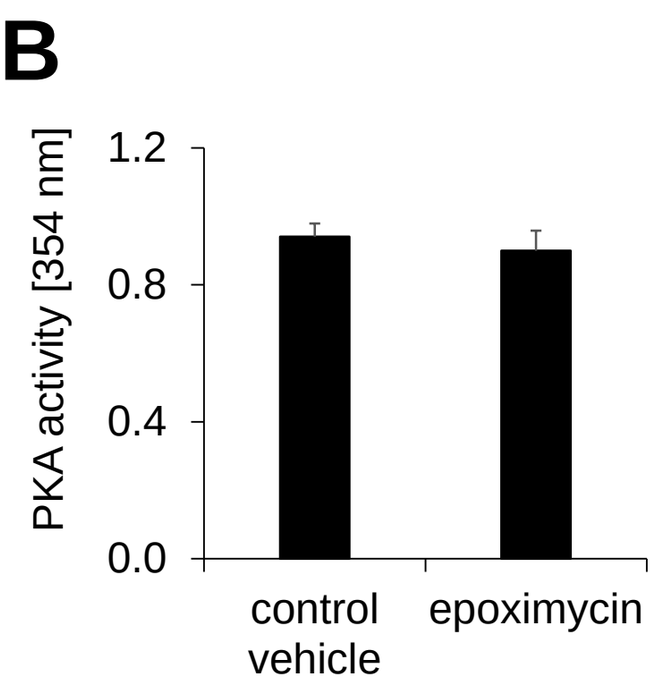

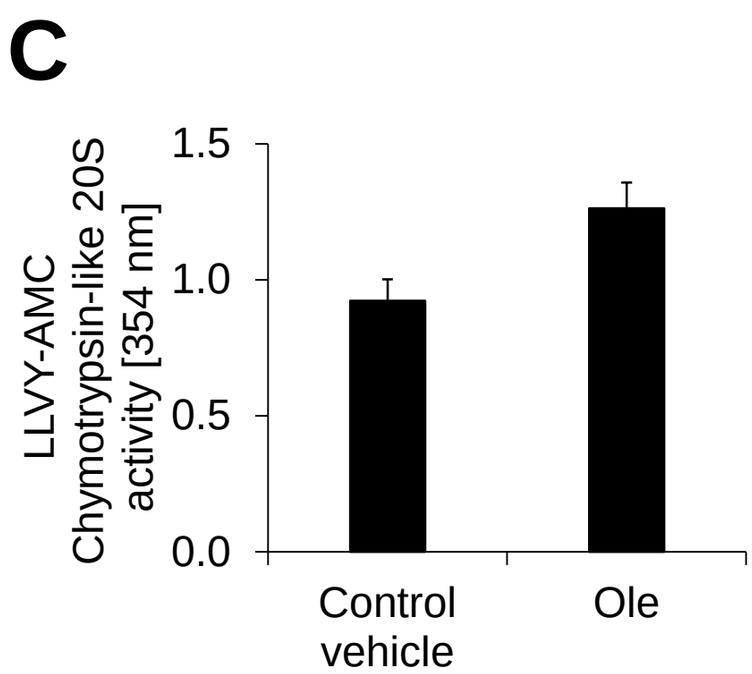

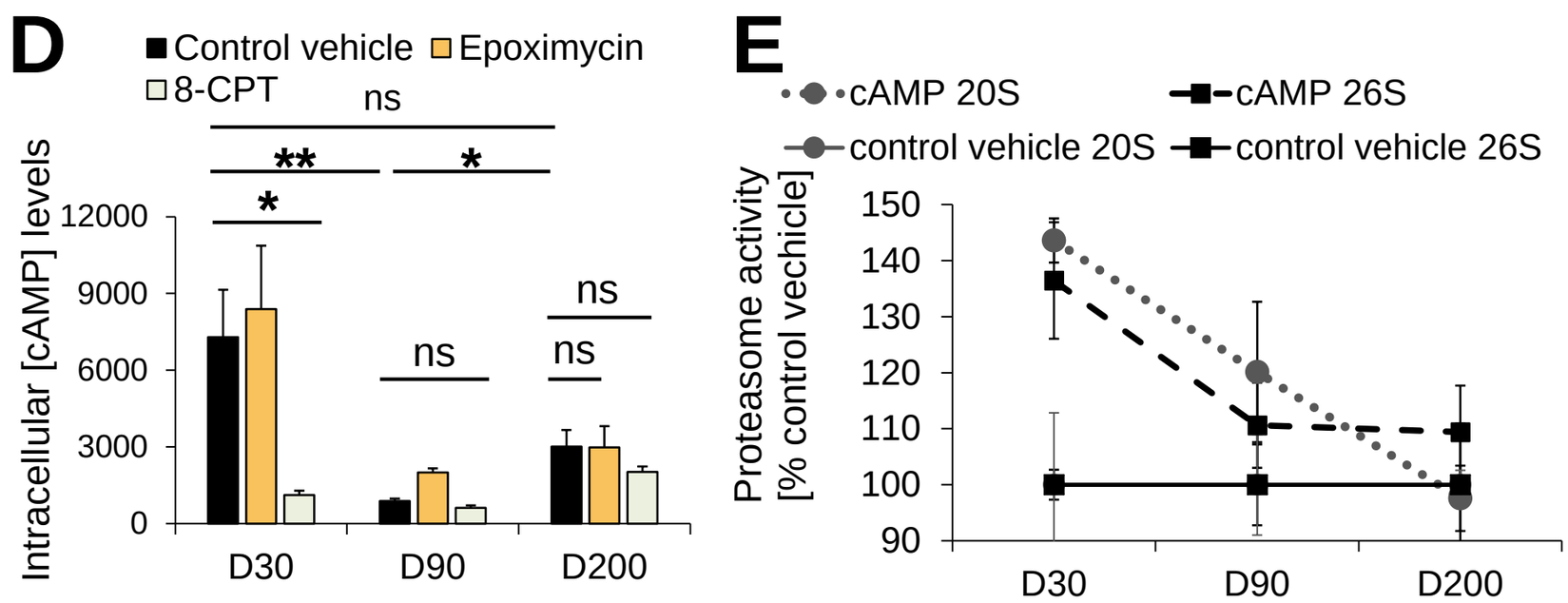

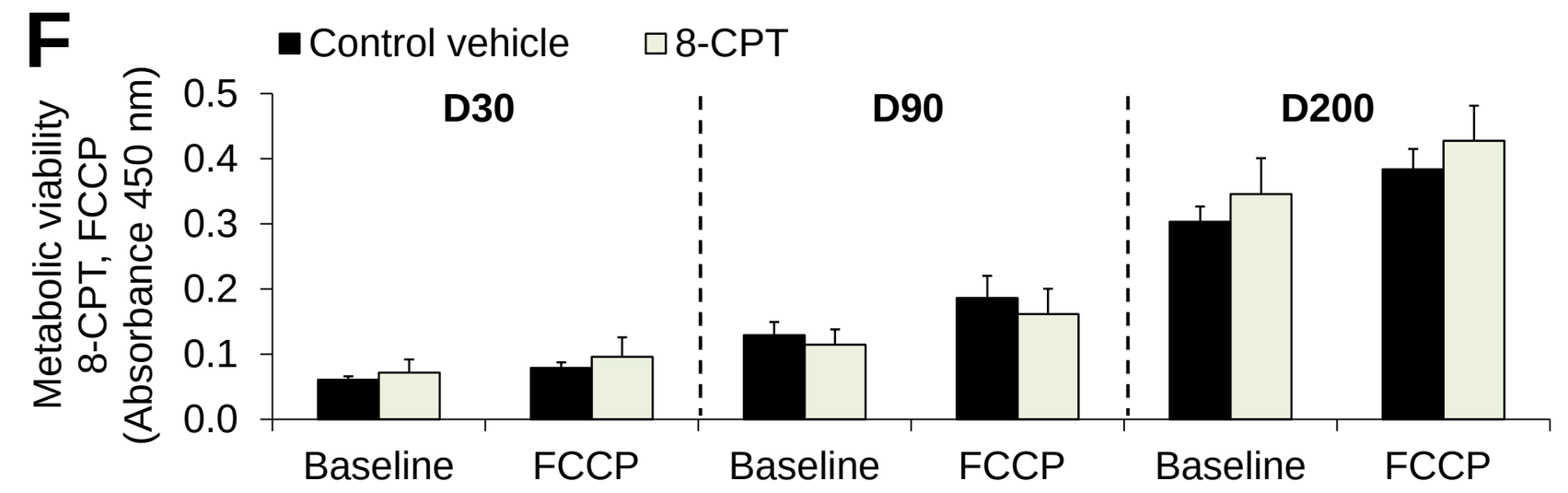

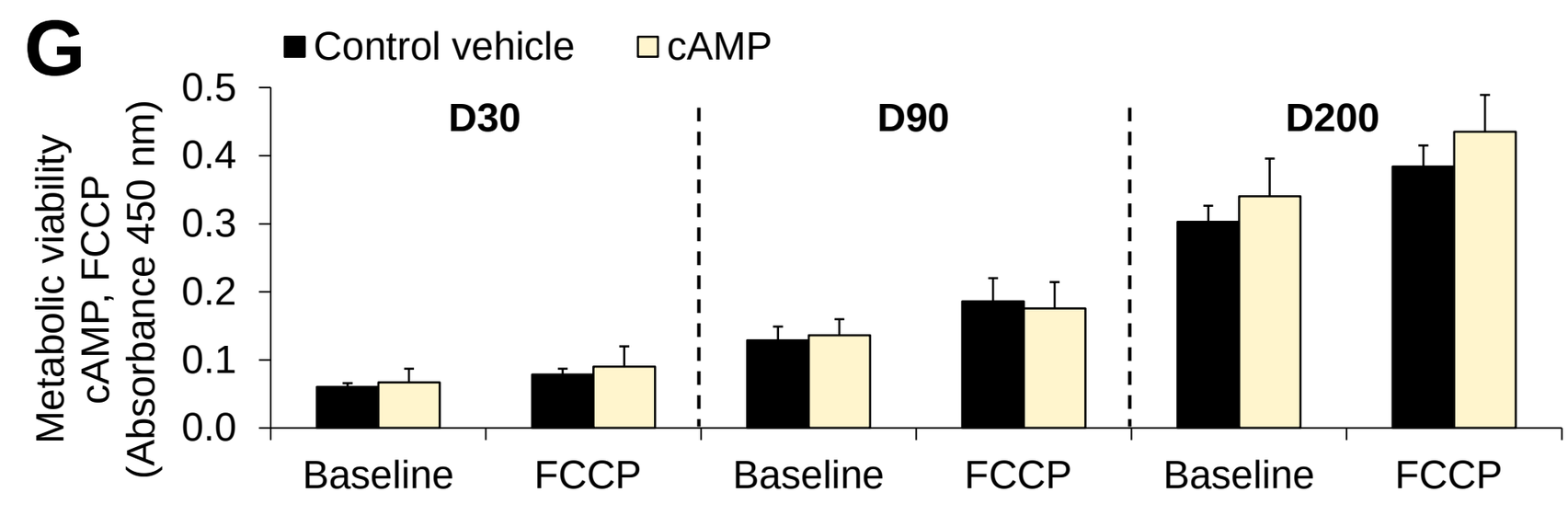

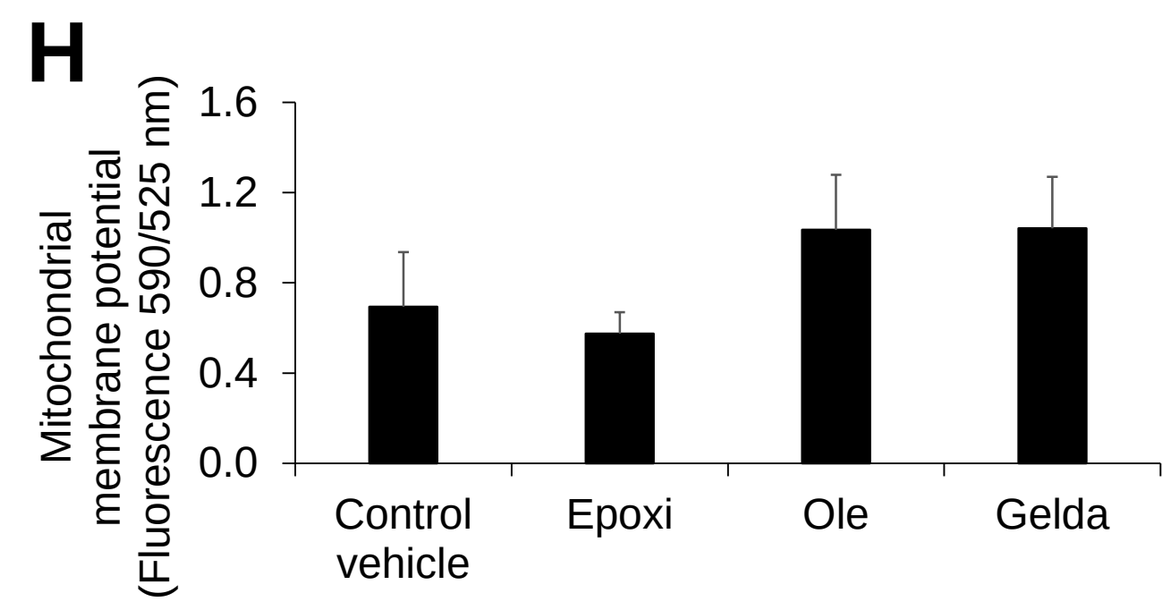

Online Figure XII

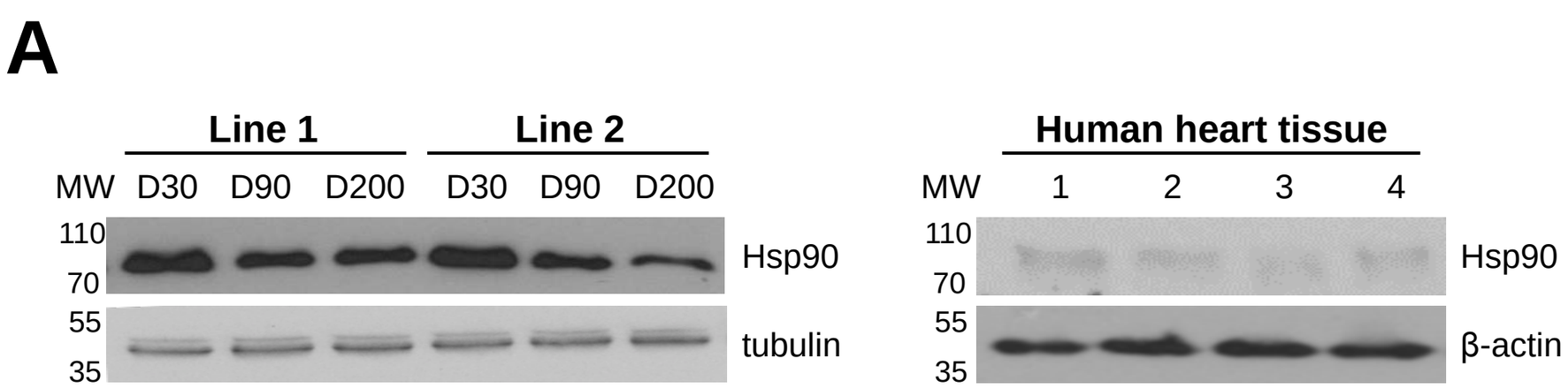

Online Figure XIII

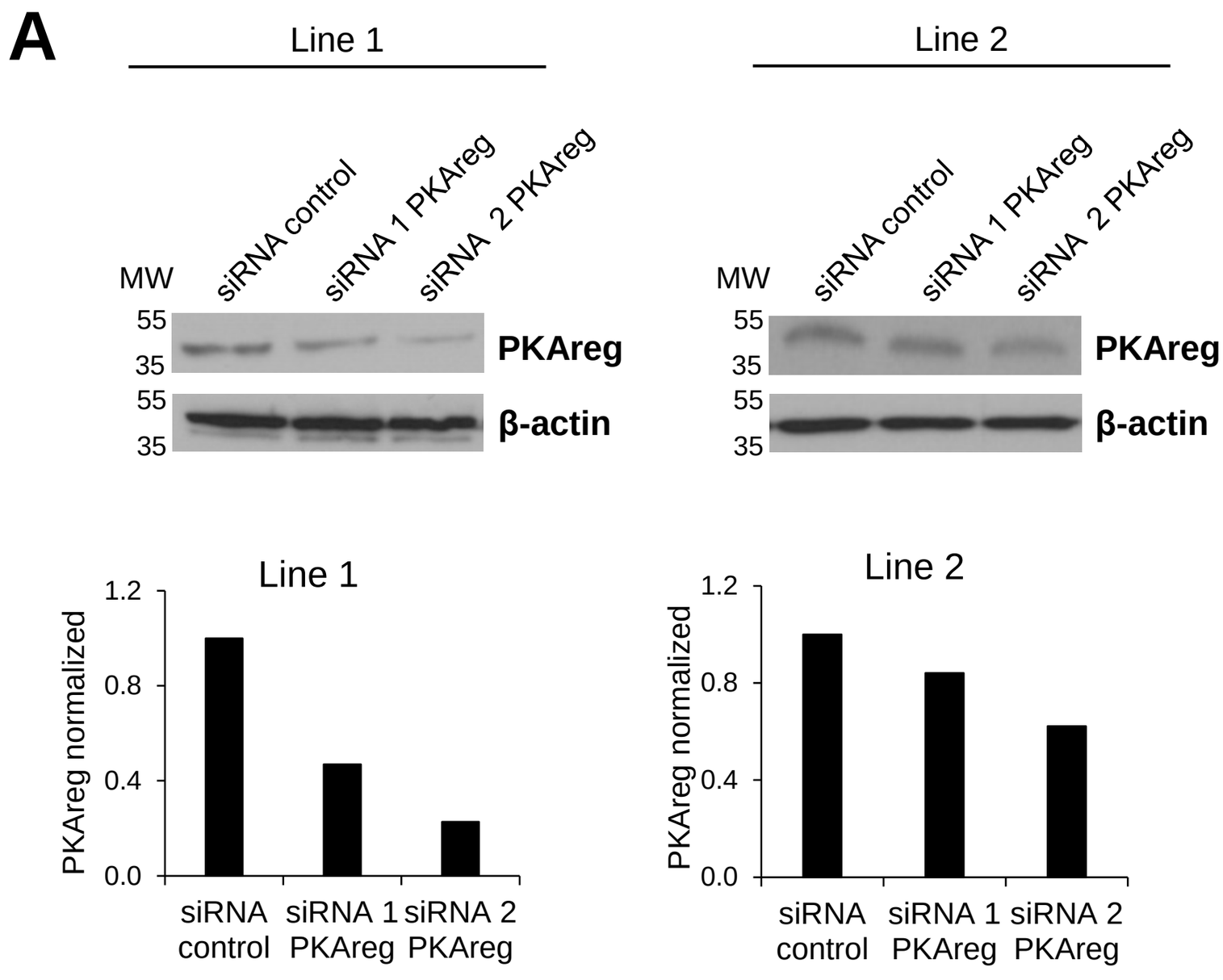

Online Figure XIV

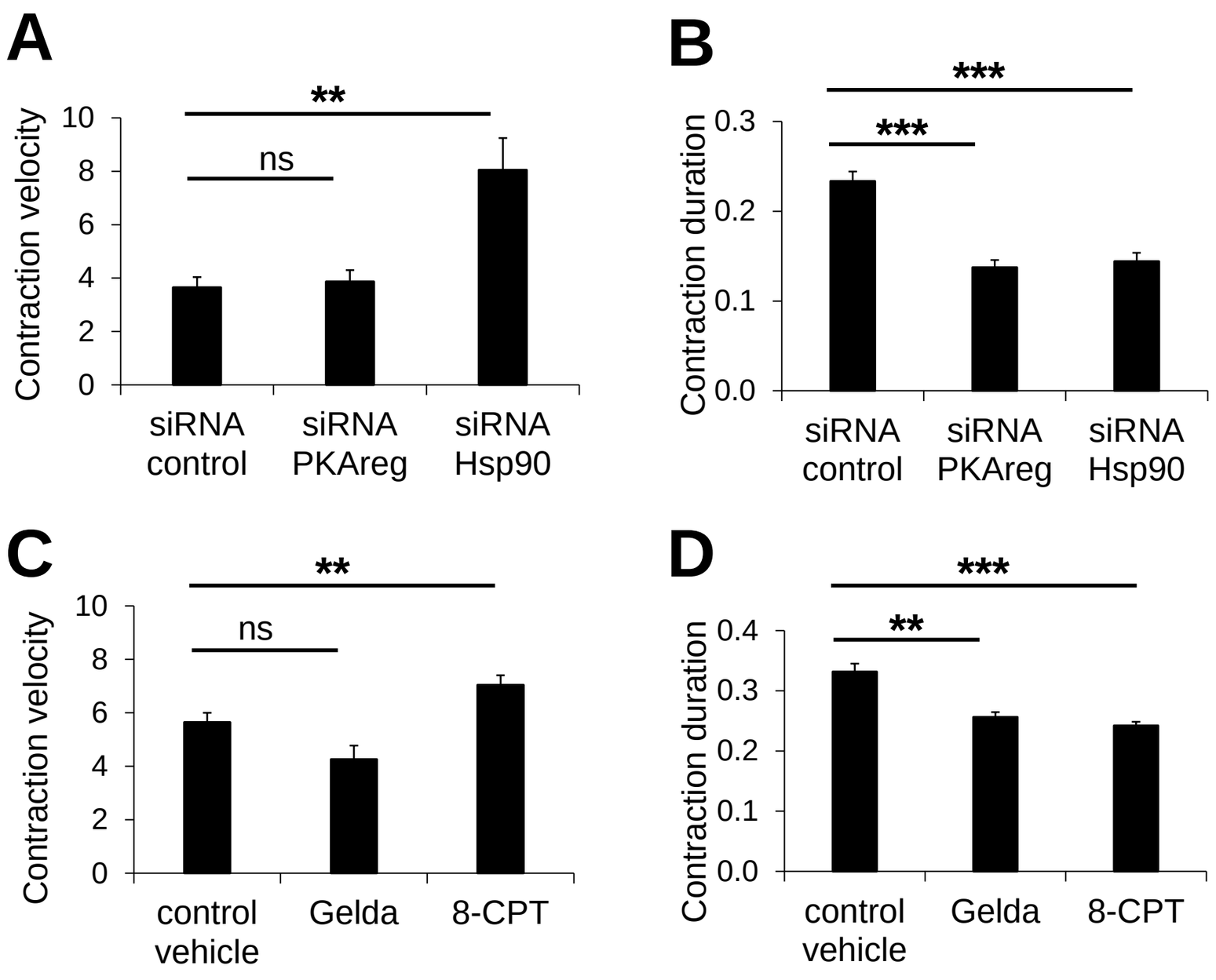

Online Figure XV

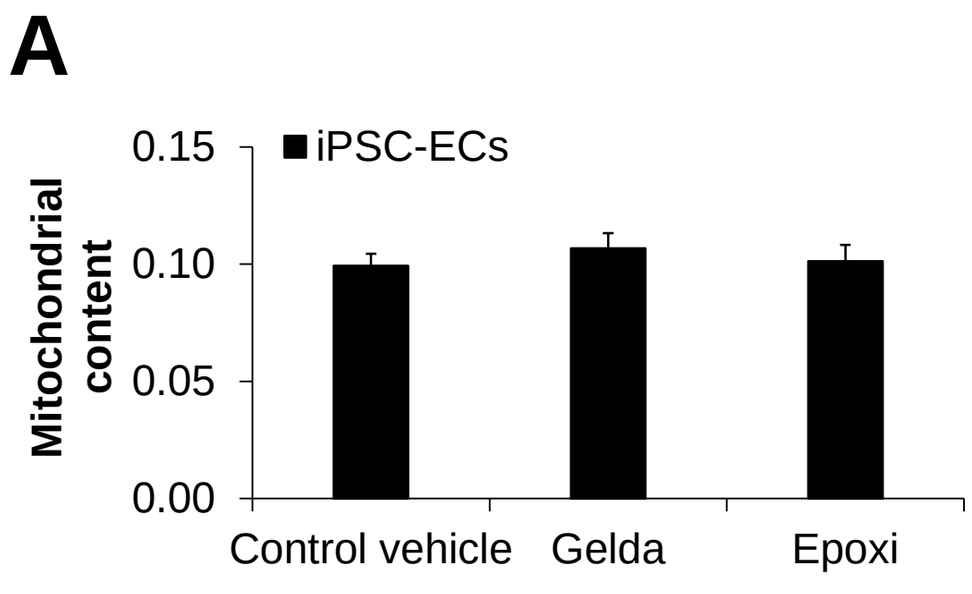

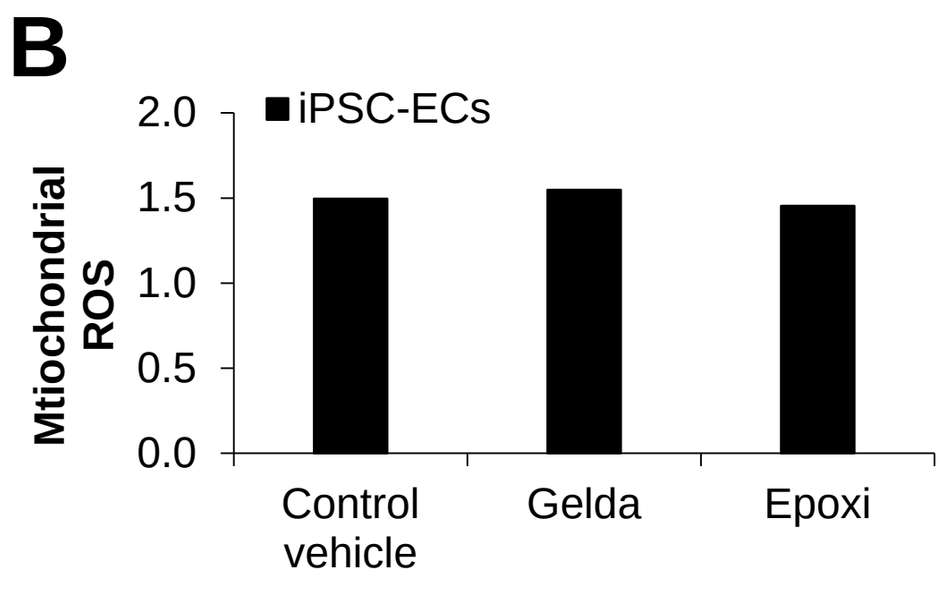

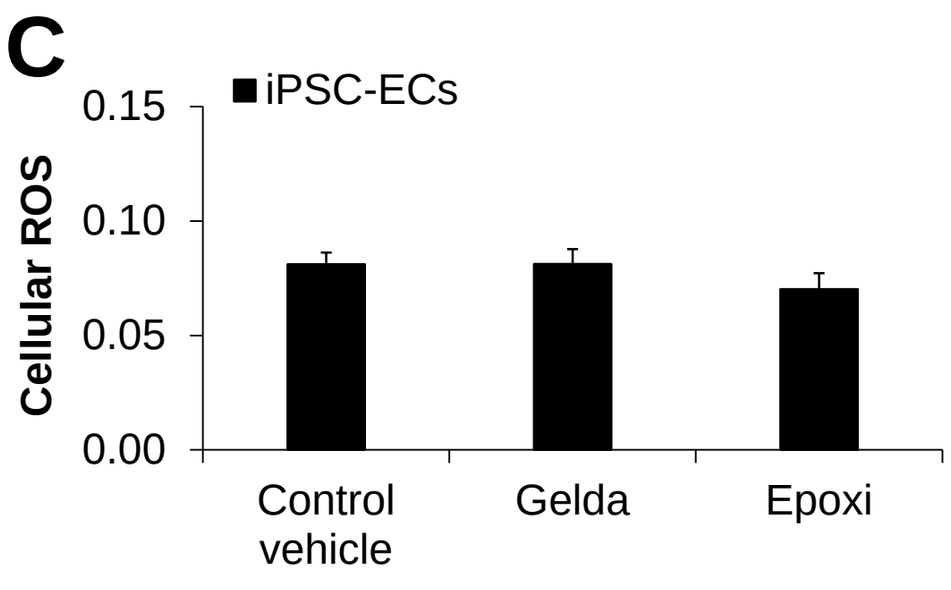

Online Table I Human qRTPCR primers (relating to Fig. 1 and Fig S2)

	Forward	Reverse
MYH6	GGAAGACAAGGTCAACAGCCTG	TCCAGTTTCCGCTTTGCTCGCT
MYH7	GGAGTTCACACGCCTCAAAGAG	TCCTCAGCATCTGCCAGGTTGT
GJA1	GGAGATGAGCAGTCTGCCTTTC	TGAGCCAGGTACAAGAGTGTGG
NFKB1	GCAGCACTACTTCTTGACCACC	TCTGCTCCTGAGCATTGACGTC
ACTN	CAGGACCGTGTGGAGCAGATTG	CAGATTGTCCCACTGGTCACAG
TNNI3	CGTGTGGACAAGGTGGATGAAG	GCCGCTTAAACTTGCCTCGAAG
GJA3	ACCGTGCTGTTCATCTTCCGCA	TGTCGTAGCAGACGTTCTCGCA
CASQ2	GCAGCAAACTGGAAGTCCAAGC	GATGTAAGGCTGGAAGTGTTCAG
ATGR1a	CCATGTTCTGACCTTCCTGGATG	CGGATTAACGCAGCTGTTGGTG
SCN5A	CAAGACCTGCTACCACATCGTG	GTCGGCATACTCAAGCAGAACC
KCNQ1	AAGACCATCGCCTCCTGCTTCT	CGGTTGAAGTGCTTCTGCCTCT
MYL2	CGGAGAGGTTTTCCAAGGAGGA	CTCTTCTCCGTGGGTGATGATG
18S rRNA	CTACCACATCCAAGGAAGCA	TTTTTCGTCACTACCTCCCCG

Online Table II Mouse qRTPCR primers (relating to Fig. S2)

	Forward	Reverse
Cx43	ACCTGACGACAGAGCAGAACTG	ACCAAGGCACTCTCCTGTAAGC
NFKB1	GCTGCCAAAGAAGGACACGACA	GGCAGGCTATTGCTCATCACAG
ACTN	TCGCCAAGTGTCAACGCTCGTT	GGTCGATGGTTTCCAGCAGCTT
TNNI3	CTCTGCCAACTACCGAGCCTAT	CGTTCCATCTCCTGCTTCGCAA
ATGR1a	GCCATTGTCCACCCGATGAAGT	ACACATTTCGGTGGATGACGGC
SCN5A	CAGACACTGATGACCAGGAAGAG	TCGGCTTCAGAGGATGTGGTCT
KCNQ1	GGAAGACCATCGCCTCCTGTTT	CGGTTGAAGTGCTTCTGCCTCT
18S rRNA	GCAATTATTCCCCATGAACG	GGCCTCACTAAACCATCCAA

Online Table III Human TaqMan probes utilized for singe-cell PCR (ThermoFisher) Relating to Fig. 2 and Online Figure IV

ACTB	ACTN	ADRB1	ATP2A2	BMP4
BMPR1A	CASQ2	CSNK1A1	FGF2	GAPDH
GATA4	GJA1	GRB2	GUSB	HAND1
HAND2	HCN4	KCNJ2	LEFTY2	MAPK14
MEF2C	MYH6	MYH7	MYL2	MYL7
MYOCD	NKX25	NODAL	NPPA	PLN
POU5F1	PPARA	PPARGC1A	PRKAA1	RYR2
SCL2A4	SCN5A	SMAD2	TBX5	TGFB2
TGFBR2	TNNC1	TNNI3	TNNT2	VCAM1
WNT1	WNT3A			

Online Table IV Pathway analysis via STRING database (Relating to Fig. 5A)

Interactor (Gene ID)	1st shell interactors	2nd shell interactors
PRKAR1A	x	
PRK	x	
PRKARCA	x	
PRKAR2B	x	
HSP90AA1	x	
PSMD4	x	
PSMD2		x
PSMD14		x
UBC	x	
PDE4D	x	